MARTIN MARIETTA ENERGY SYSTEMS LIBRARIES
3 4456 0250473 3

ORNL-2529
Physics and Mathematics

COMPARISON OF THEORETICAL AND EXPERIMENTAL FILTERED X-RAY SPECTRA

J. C. Villforth
R. D. Birkhoff
H. H. Hubbell, Jr.

OAK RIDGE NATIONAL LABORATORY
operated by
UNION CARBIDE CORPORATION
for the
U.S. ATOMIC ENERGY COMMISSION

CENTRAL RESEARCH LIBRARY
DOCUMENT COLLECTION
LIBRARY LOAN COPY
DO NOT TRANSFER TO ANOTHER PERSON
If you wish someone else to see this document, send in name with document and the library will arrange a loan.

Printed in USA. Price $2.25 cents. Available from the

Office of Technical Services
U. S. Department of Commerce
Washington 25, D. C.

LEGAL NOTICE

This report was prepared as an account of Government sponsored work. Neither the United States, nor the Commission, nor any person acting on behalf of the Commission:

A. Makes any warranty or representation, express or implied, with respect to the accuracy, completeness, or usefulness of the information contained in this report, or that the use of any information, apparatus, method, or process disclosed in this report may not infringe privately owned rights; or

B. Assumes any liabilities with respect to the use of, or for damages resulting from the use of any information, apparatus, method, or process disclosed in this report.

As used in the above, "person acting on behalf of the Commission" includes any employee or contractor of the Commission to the extent that such employee or contractor prepares, handles or distributes, or provides access to, any information pursuant to his employment or contract with the Commission.

ORNL-2529

Contract No. W-7405-eng-26

HEALTH PHYSICS DIVISION

COMPARISON OF THEORETICAL AND EXPERIMENTAL FILTERED X-RAY SPECTRA

J. C. Villforth
R. D. Birkhoff
H. H. Hubbell, Jr.

Submitted as a thesis to the Faculty of the Graduate School of Vanderbilt University in partial fulfillment of the requirements for the degree of Master of Science in physics.

DATE ISSUED

JUL 1 1958

OAK RIDGE NATIONAL LABORATORY
Oak Ridge, Tennessee
operated by
UNION CARBIDE CORPORATION
for the
U.S. ATOMIC ENERGY COMMISSION

MARTIN MARIETTA ENERGY SYSTEMS LIBRARIES

3 4456 0250473 3

ACKNOWLEDGMENTS

The authors take pleasure in acknowledging the assistance of the following persons: V. A. McKay of the Instrument Division, ORNL, for mounting the crystal; J. A. Harter and H. F. Holzer of the Health Physics Division for assistance with the electronics; and F. H. W. Noll of Berea College for assistance in the preliminary phases of the work and for his suggestions on the manuscript.

J. C. Villforth, in particular, wishes to extend his appreciation to the United States Air Force Institute of Technology, Air University, for making available the opportunity to do this work, and to Dr. E. E. Anderson, ORNL, for her help in coordinating the program with the United States Air Force.

TABLE OF CONTENTS

		Page
	Acknowledgments	ii
	List of Tables	iv
	List of Figures	v
I.	Introduction	1
II.	The Scintillation Spectrometer	5
III.	Corrections of the Scintillation Spectrometer Data	7
IV.	Calibration of the Scintillation Spectrometer	15
V.	Correction of the X-ray Spectra	46
VI.	Kramers' Theory	54
VII.	Absorption Method	62
VIII.	Summary and Discussion	66
	Appendix	70
	Bibliography	74

LIST OF TABLES

		Page
I.	Fluorescent Radiators Used for Spectrometer Calibration	39
II.	Summary Data for Calibration	45
III.	Kilovolt Settings and Standard Filtration	47
IV.	Comparison of the Average Energy, Most Probable Energy and the Effective Energy	65

LIST OF FIGURES

		Page
1.	Absorption Coefficients for Iodine	8
2.	Schematic Diagram of the Apparatus	16
3.	Isotopic Decay Schemes	19
4.	Cerium^{141} Spectrum	20
5.	Thulium^{170} Spectrum	21
6.	Osmium^{191} Spectrum	22
7.	Mercury^{203} Spectrum	23
8.	Pulse Height as a Function of Gamma Ray Energy	25
9.	Gaussian Representation of Data, 145 Kev Cerium^{141} Gamma Peak	27
10.	a^2 as a Function of Gamma Ray Energy	28
11.	Comparison of Experimental Data with Normalized Gaussian Curves	29
12.	Change in Resolution of the Platinum K X-ray Spectra as a Result of K_β Contribution	32
13.	Resolution Correction Factors for the Experimental K X-ray Resolutions	33
14.	Comparison of Filtered and Unfiltered Fluorescent K X-ray Spectra of Uranium	36
15.	Comparison of Filtered and Unfiltered Fluorescent K X-ray Spectra of Uranium with curves normalized to the Same Peak Count Rate	37
16.	Schematic Diagram of Fluorescent X-ray Apparatus	41
17.	Pulse Height as a Function of Photon Energy	42
18.	a^2 as a Function of Photon Energy	44

LIST OF FIGURES CON'T

		Page
19.	Normalized Gaussians	49
20.	Product of the Normalized Gaussians and the 250 Kev Experimental Spectrum	50
21.	The Effect of the First Iteration on the 250 Kev Experimental Spectrum	52
22.	Comparison of Corrected Experimental Values with the Theoretical Kramers' Distribution for the 250 Kev Spectrum	56
23.	Comparison of Corrected Experimental Values with the Theoretical Kramers' Distribution for the 200 Kev Spectrum	57
24.	Comparison of Corrected Experimental Values with the Theoretical Kramers' Distribution for the 150 Kev Spectrum	58
25.	Comparison of Corrected Experimental Values with the Theoretical Kramers' Distribution for the 100 Kev Spectrum	59
26.	Comparison of Corrected Experimental Values with the Theoretical Kramers' Distribution for the 50 Kev Spectrum	60
27.	Comparison of Corrected Experimental Values with the Theoretical Kramers' Distribution for the 30 Kev Spectrum	61
28.	Absorption Curves for the 250 Kev Spectrum	63

ABSTRACT

Spectral distributions of filtered X-ray beams have been taken for six X-ray tube voltages from 30 Kev to 250 Kev with a sodium iodide scintillation spectrometer. The spectrometer was calibrated for energy response and resolution with gamma rays and K X-rays from radioactive isotopes as well as K X-rays from fluorescent radiators. Since the spectrometer failed to resolve the K series lines, a better estimate of the resolution constant was obtained by filtering out the K_β lines with an absorber of slightly lower Z than the radiator. For example, in the case of the K lines of uranium filtering with thorium reduced the width of the K lines profile from 36% greater to only 6% greater than the value expected for the profile of a monoenergetic line. Calculated correction curves permitted a determination of the resolution constant from the observed profiles of either the filtered or unfiltered K series. Some of the filters and radiators were made by casting appropriate chemical compounds in plastic.

The effect of the scintillation spectrometer resolution was removed from each experimental spectrum by an iteration method. Two iterations were necessary in order to obtain a system which when combined with the spectrometer line profile would yield the experimental distribution within an error of about 4%. Corrections were also made to the iterated spectra

where necessary to reduce the effect of the loss of photons from iodine K escape and lack of complete absorption in the crystal.

The corrected experimental spectra were compared to spectra calculated from Kramers' distribution and the absorption in the filters. Agreement was good except for the 30 Kev spectra, which was displaced slightly, due probably to the difficulties found in calibrating the spectrometer at low energy. The average energies and most probable energies agreed within 3%. In addition to these values, the effective energies were obtained by the absorption method using a standard air chamber. These values were within 3.5% of the corrected experimental average energy except for the two low energy spectra which differed by as much as 10%.

I. INTRODUCTION

Although X-rays have been under intensive use and study for over sixty-two years, techniques for their accurate analysis have only recently been developed. Along with improvements in techniques has come an increased interest in medical diagnostic X-ray exposures. This is primarily due to the realization by the medical profession that the public now receives an unnecessarily high exposure from routine medical X-ray examinations. In 1956, the National Academy of Sciences Committee on Genetic Effects of Atomic Radiation recommended that, "... the general public of the United States be protected, by whatever controls may prove necessary, from receiving a total reproductive lifetime dose of more than 10 roentgens of man-made radiation to the reproductive organs."[1] The Committee now estimates the dose from medical examinations as between 1.0 and 5.0 roentgens. Lapp[2] also has made an estimate of the thirty-year gonad dose as 10 roentgens. One of the first steps in an attempt to reduce this quantity is an accurate measure of the X-ray spectral distribution. The methods for determining this distribution are the basis for the present work. Accurate X-ray spectral analysis is also needed for precise biological experiments and for the calibration of radiation detection equipment.

---

1 "The Biological Effects of Atomic Radiation," Report of the Committee on Genetic Effects, National Academy of Sciences - National Research Council, Washington, (1956), p. 29 of Summary Reports.

2 Schubert, J., and Lapp, R. E., RADIATION: WHAT IT IS AND HOW IT AFFECTS YOU, (The Viking Press, Inc., New York, 1957) p. 195.

The techniques and equipment now used conventionally to measure X-ray spectra, while satisfactory for the use to which they were put, have their limitations. Ehrlich[3] states that, "No absolute, fully corrected experimental data have ever been published, and no technique has been developed for a routine investigation of spectra from commercial X-ray tubes." It is hoped that the method described in this paper will be a step in overcoming the problem.

One of the earliest attempts at measuring continuous X-ray spectra was the work of Hull[4] using the crystal diffraction spectrometer. Further work utilizing a modification of this method was reported by Webster,[5] Ulrey,[6] and Kulenkampff.[7] Although the crystal diffraction spectrometer has excellent resolution, it is limited to comparatively low energies, and is a relatively poor instrument for measuring absolute energies. It is also complicated to operate and is not portable.

A less elaborate but more commonly used method for describing X-ray spectra is by use of absorption data. When an X-ray beam is required to pass through successively greater thicknesses of material, the resultant absorption may be used to give an estimate of the X-ray spectrum. Duane,[8] Kulenkampff,[9] and Nicholas[10] used this procedure

---

3 Ehrlich, M., J. Research Natl. Bur. Standards, 54, No. 2, 107 (1955).

4 Hull, A. W., Gen. Elec. Rev., 19, 603 (1916).

5 Webster, D. L., Phys. Rev., 9, 220 (1917).

6 Ulrey, C. T., Phys. Rev., 11, 401 (1918).

7 Kulenkampff, H., Ann. Physik, 69, 548 (1922).

8 Duane, W., Proc. Nat. Acad. Sci. U. S., 13, 662 (1927).

9 Kulenkampff, H., Ann. Physik, 87, 597 (1928).

10 Nicholas, W. W., J. Research Natl. Bur. Standards, 2, 837 (1929).

on X-ray beams emanating from thin targets. Silberstein[11] showed that it is possible to determine mathematically the spectral distribution based on the absorption data. Bell,[12] Taylor,[13] and Jones[14] modified Silberstein's method slightly, using the half-value layer of radiation and peak kilovoltage of the X-ray tube. Greening[15] applied the absorption method to include distributions containing characteristic lines as well as the continuous spectrum. More recently, Greenfield[16] and Wang[17] used Laplace transforms to arrive at a continuous energy distribution from the absorption curves.

A more direct and detailed method of analysis of X-ray spectra than has been obtainable in the absorption method was possible with the advent of the scintillation spectrometer. In 1945 it became apparent that if a scintillating crystal were coupled to a photomultiplier tube, the resulting combination would be a very efficient and sensitive device for measuring radiation.[18] The first scintillation materials were the organic phosphors such as napththalene and anthracene.[19] These materials have their limitations: low

---

11 Silberstein, L., J. Opt. Soc. Am., 22, 265 (1932).

12 Bell, G. E., Brit. J. Rad., 9, 680 (1936).

13 Taylor, L. S., Radiology, 29, 22 (1937).

14 Jones, D. E. A., Brit. J. Rad., 13, 95 (1940).

15 Greening, J. R., Brit. J. Rad., 20, 71 (1947).

16 Greenfield, M. A., Specht, R. D., Kratz, P. M., and Hand, K., J. Opt. Soc. Am. 42, 6 (1952).

17 Wang, P. K. S., Brit. J. Rad., 30, 153 (1957).

18 Blaw, M., and Dreyfus, B., Rev. Sci. Ins., 16, 245 (1945).

19 Bell, P. R., Phys. Rev., 73, 1405 (1948).

density, low atomic number, and relatively weak scintillations. Hofstadter[20,21] pointed out that these difficulties could be overcome with the alkali halide phosphors, such as thallium-activated sodium iodide. In recent years, much successful work has been done in spectral analysis of gamma rays using the NaI(Tl) counter. Work has been done elsewhere with this technique on X-rays from commercial X-ray machines.[3,22,23,24] It is the purpose of this work to make such X-ray energy determinations for heavily filtered X-ray beams and to compare the results obtained by the several methods.

---

[20] Hofstadter, Phys. Rev. 75, 796 (1949).

[21] Hofstadter, R., Phys. Rev. 74, 100 (1948).

[22] Ramm, W. J., and Stein, M. N., Phys. Rev., 92, 1081A (1953).

[23] Cormack, D. V., Till, J. E., Whitmore, G. F. and Johns, H. E., Brit. J. Rad., 28, 605 (1955).

[24] Ehrlich, M., Radiation Research, 3, 223A (1955).

II. THE SCINTILLATION SPECTROMETER

The scintillation spectrometer operates on the principle that there is a direct proportionality between the energy absorbed in the crystal and the light produced by the crystal. The light emitted by the crystal ejects photoelectrons from the cathode of the photomultiplier tube by the photoelectric process. These photoelectrons after amplification produce a pulse at the anode of the photomultiplier tube whose height is proportional to the energy of the incident photons.

The molecules of the scintillation crystal, excited by the passage of radiation return to their normal or ground state with the emission of light. Part of this light is collected at the photocathode of the photomultiplier, causing the ejection of electrons. These electrons are accelerated to the second electrode (dynode), where a larger number of electrons are produced, which, in turn, are accelerated to the next dynode. This process may take place nine or more times, depending on the number of stages of the photomultiplier tube. The result is a current pulse at the anode with an amplitude proportional to the light intensity emitted from the crystal. This pulse is amplified, fed to the pulse height analyzer, and then to a scaler where it is recorded.

The thallium-activated sodium iodide scintillation counter has proven exceedingly useful in detecting low energy electromagnetic radiation. The high atomic number (for iodine, Z = 53) of the crystal

results in high absorption due to the photoelectric process, when photons of energy less than 0.5 Mev are incident on the crystal. Use of NaI(Tl) thus reduces the energy lost from the crystal by the escape of the Compton photons.

III. CORRECTIONS OF THE SCINTILLATION SPECTROMETER DATA

The calculation of an energy distribution from an observed experimental spectrum involves a thorough knowledge of the processes that occur in the spectrometer.

In following the chain of events from the time the incident photon strikes the crystal to the time the amplified voltage pulse reaches the anode, several factors are found which cause the observed distribution to differ from the true distribution. Careful analysis yields corrections which can be applied to the pulse height distribution in order to find the original distribution incident on the crystal. Absorption between the X-ray tube and the detector is neglected since most spectral analysis is concerned with the energy distribution at the point of detection and not at the source.

As the photon passes through the crystal, it may be removed from the beam by photoelectric effect, Compton effect, or pair production. The probability of any one reaction, which is proportional to the cross section, depends on the energy of the incident beam and the atomic number of the absorber. For example, the photon energy necessary for pair production is 1.02 Mev. Since the energies used in this experiment are less than 0.3 Mev, pair production does not occur. The cross sections for the reactions at various energies are shown for iodine (84.7% by weight of the NaI) in Figure 1.[25] In the Compton scattering process, a photon is deflected with a reduction in energy, and an

---

[25] Grodstein, G. W., "X-Ray Attenuation Coefficients from 10 Kev to 100 Mev," Natl. Bur. Standards Circ. 583 (1957).

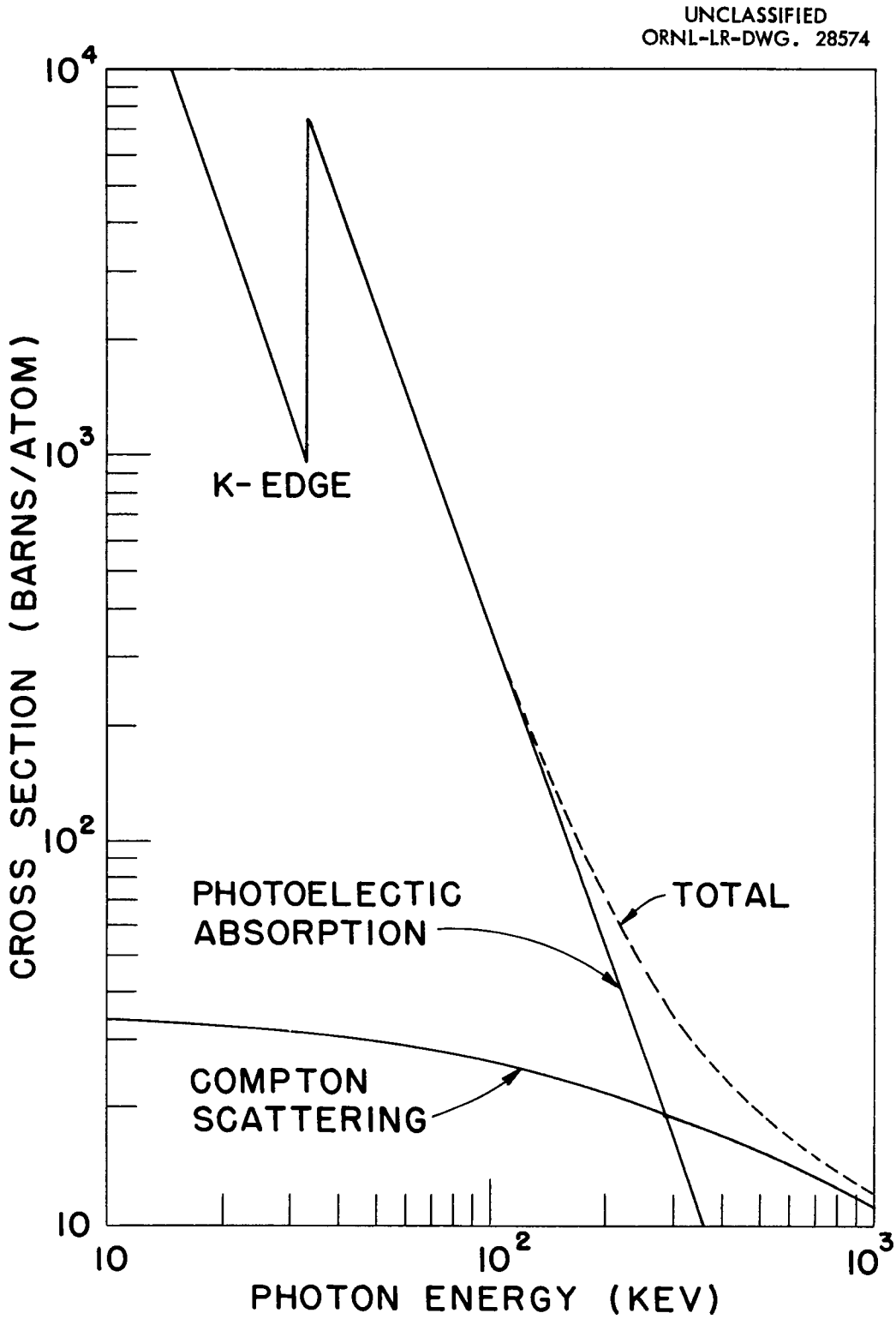

Figure 1. Absorption Coefficients for Iodine.

atomic electron recoils out of the atom. If none of the radiation scattered by the Compton process leaves the crystal, the light emitted is equal to that emitted in the photoelectric process and the pulse in the external circuit is the same as that observed in the photoelectric process. If the scattered Compton photon escapes the crystal without interacting, the resultant pulse is reduced by the amount of the Compton energy which is lost.* If this incident radiation is not monochromatic, then the Compton continuum becomes complex and difficult to evaluate.

Figure 1 illustrates that the Compton cross section is small relative to the total absorption cross section at low energies, i.e., less than 7% at 100 Kev. No corrections were made for the loss of photons scattered by the Compton process in correcting the pulse height spectrum for it was seen that the Compton scattered photons did not contribute more than 2% of the total counting rate as illustrated in Figure 22.

Of the three processes of interaction of gamma or X-rays with matter, the photoelectric absorption is the most significant at low energies in the NaI(Tl) scintillation counter. The photoelectric cross section varies as approximately the fifth power of atomic number

---

* The maximum size of the pulse in which the Compton photon escapes corresponds to the scattering of the electron in a direction toward the X-ray source. In this situation the escaping photon has minimum energy. The energy absorbed in the crystal is equal to the energy of the Compton electron and may be represented as:

$$E_{Max} = \frac{1}{1 + \frac{.51}{2E}}$$

where E is the energy in Mev.

and inversely as the seven-halves power of the energy.[26] The high atomic number of iodine in the sodium iodide crystal makes it more advantageous than the organic phosphors for detecting X-radiation. In the photoelectric process, the energy is completely absorbed and the light produced is proportional to the photon energy. Thus the pulse height distribution resembles closely the incident photon spectrum.

In the photoelectric process at energies above the K absorption edge, the photon interacts in the majority of cases with the K-shell electron. The photoelectron leaves the K-shell with an energy equal to the energy of the incident photon less the binding energy of the electron, and is absorbed in the crystal. A K X-ray is given off having an energy equal to the difference in binding energy of the K- and L-shell electrons (28.4 Kev for iodine). This photon is usually absorbed by subsequent photoelectric processes. If the interaction takes place near the edge of the crystal and the X-ray escapes from the crystal, then the energy will be equal to the energy of the incident radiation less the energy of the iodine K X-ray. When an energy distribution of X-rays falls on the crystal, the resulting spectrum will reveal a subsidiary distribution of similar pattern to the original distribution only of less intensity and displaced from it by 28.4 kilovolts. The intensity of this "iodine escape peak" will

---

[26] Heitler, W., THE QUANTUM THEORY OF RADIATION, (Oxford Univ. Press, 1954) Third Edition, p. 207.

depend on the size of the scintillation crystal and the geometry of the system. A well-collimated beam incident perpendicular to the crystal will have a smaller escape peak than an uncollimated source close to the crystal, since there will be greater probability for the quanta to escape in the system with poorer geometry. The iodine K-escape data have been tabulated for systems of various geometries.[27,28] Since the escape peak is not a real part of the incident energy spectrum, but an experimental anomaly, corrections should be made to remove it from the spectrum where it is significant. The values listed in the literature were used to make this correction.

Even though NaI(Tl) has a large total absorption cross section for a finite crystal, it is possible that a photon incident on the crystal will not interact at all. The crystal used in this experiment was 2.62 cm high and resulted in 99.5% and 93.6% absorption at 150 Kev and 200 Kev respectively.

The correction factors for Compton continuum, iodine escape and total absorption are the results of the interactions or lack of interactions of the incident photons with the crystal detector. These are small corrections as compared to the distortions that originate in the photomultiplier tube. The correction of the distortion has been achieved by other workers with a system of matrix inversion involving

---

[27] Axel, P., BNL-271(T-44), Brookhaven Nat. Lab., Upton, N. Y., (1953).

[28] McGowan, F. K., Phys. Rev., 93, 163 (1954).

the use of a digital computer.[29,30] While this method possesses certain advantages, an alternative iterative method is used here.

To understand the method of analysis of the photomultiplier distortion, it is necessary to understand the processes that take place inside the photomultiplier tube. The light that emanates from the excited molecules in the scintillation phosphor releases electrons from the photocathode by the photoelectric process. The number of photoelectrons emitted depends on the intensity of the light reaching the photocathode and this varies depending on the location of the scintillation in the crystal, the transparency and the homogeneity of the crystal, and the type of reflector surrounding the crystal. The statistical fluctuations in the small number of photoelectrons emitted from the photocathode result in an approximate Gaussian distribution in size of the pulses reaching the first dynode. The electrons are then accelerated to the successive dynodes where successively larger numbers of electrons are produced. If the potential between dynodes fluctuates or if the electron stream from the dynodes is not properly focused then there will be an additional variation in the number of electrons reaching the anode and thus a further variation in the size of the current pulses.[31] A complete discussion of these effects is made by Breitenberger.[32] The result

---

29 Beach, L. A., Theus, R. B., and Faust, W. R., NRL Rep. 4277 (1953).

30 Ehrlich, op. cit., (footnote 3).

31 Sharpe, J., NUCLEAR RADIATION DETECTORS, (John Wiley and Sons, Inc., New York, 1955) pp. 101-107.

32 Breitenberger, E., PROGRESS IN NUCLEAR PHYSICS, (Frisch ed. - Pergammon Press, New York, 1955) pp. 54-94.

of these fluctuations is that for repeated absorptions in the crystal of the same amount of energy, the corresponding pulses at the anode will fluctuate in size, even though on the average, the pulses will be proportional to the average light absorbed.

The expression for a normalized Gaussian can be written as:

$$P(n,r) = \frac{1}{\sqrt{2\pi r}} \exp\left[- \frac{(n-r)^2}{2r} \right] \qquad (1)$$

where P(n,r) is the probability of n photoelectrons being emitted from the photocathode and r is the average number emitted. This expression can be written in terms of counting rate of pulses of height H or of energy E[33] assuming

$$P(n,r)dn = G(h,H)dH = L(E,E')dE' \qquad (2)$$

The pulse height distribution and apparent energy distribution are then, from equations 1 and 2,

$$G(h,H) = \frac{\alpha}{a\sqrt{\pi}} \exp\left[- \frac{\alpha^2}{a^2} (h-H)^2 \right] \qquad (3)$$

and

$$L(E,E') = \frac{1}{a\sqrt{\pi}} \exp\left[- \frac{(E-E')^2}{a^2} \right] \qquad (4)$$

where α is a constant of conversion from pulse height units to energy, and takes the units Kev/phu. The parameter "a" is proportional to the square root of the energy and is equal to the half-width of the distri-

---

33 Johnston, L. W., Birkhoff, R. D., Cheka, J. S., Hubbell, H. H., Jr., and Saunders, B. G., ORNL-2298, Oak Ridge, Tennessee, (1957); and Rev. Sci. Instr. 28, 765 (1957).

bution at 1/e times the maximum counting rate. The resolution of the instrument can thus be expressed by the parameter "a".

Several experimenters have attempted to remove the distortions due to the Gaussian distribution of pulse heights.[34-37] Freedman, et. al.,[38] have suggested that the distortions of a pulse height distribution due to the Gaussian "smearing" can be removed by an iterative procedure. Such a procedure requires no elaborate electronic computer, is readily adapted to a desk calculator, and was used in this research.

---

[34] Madansky, L., and Rasetti, F., Phys. Rev. 83, 187 (1951).

[35] Ehrlich, op. cit., (footnote 3).

[36] Liden, K., and Starfelt, N., Arkiv för Fysik, 7, 427 (1954).

[37] Johansson, S. A. E., Arkiv för Fysik 3, 533 (1952).

[38] Freedman, M. S., Novey, T. B., Porter, F. T., and Wagner, F., Rev. Sci. Instr., 27, 716 (1956). A similar technique was suggested by Owen, G. E. and Primakoff, H., Phys. Rev. 74, 1406 (1948).

IV. CALIBRATION OF THE SCINTILLATION COUNTER

A careful calibration of the scintillation spectrometer is necessary in order to permit conversion of observed counts per minute versus pulse height to an X-ray energy distribution. Two basic calibrations are needed: 1) pulse height versus energy, and 2) resolution versus energy. The calibration procedure was performed in two steps. The first step was to make a rough approximation of these two calibrations, using data from three isotopes. The second step resulted from the realization that the three isotopes did not provide enough information, especially at lower energies. Therefore, additional calibration data from fluorescent X-rays and isotopic X-rays were obtained to supplement the original data.

The X-ray source and the scintillation spectrometer are shown in Figure 2. The NaI(Tl) crystal was 2.62 cm high and 3.63 cm in diameter, and was surrounded with magnesium oxide and covered with aluminum foil to seal out moisture. An RCA 6199 photomultiplier was selected on the basis of the lowest signal to noise ratio of twelve tubes available in stock. The tube and crystal assembly was protected from external magnetic and electrostatic sources by a "Mu metal" shield. This unit was placed in a lead "pig" made from lead brick and covered with a lead plate 1.7 cm thick and with a 0.6 cm diameter collimation hole centered over the crystal. The use of a well-collimated beam increases the efficiency of the crystal by reducing the loss of the Compton scattered photons and the iodine escape K X-ray photons. The pulse at the tube anode was

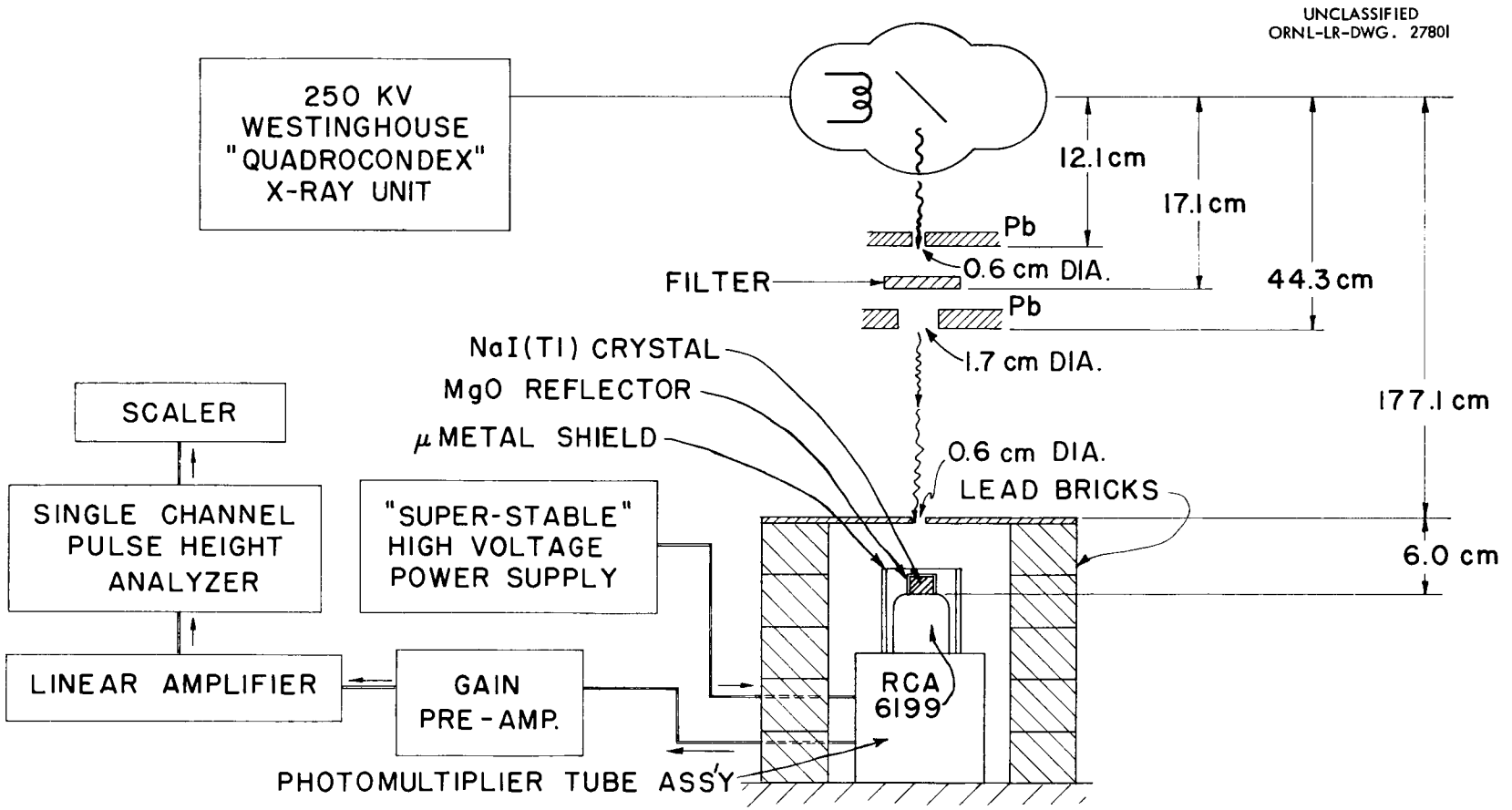

Figure 2. Schematic Diagram of the Apparatus.

amplified by a pre-amplifier and then by a linear amplifier, Atomic Instrument Company Model 218. The pulse height spectrum was measured with a single channel pulse height analyzer (Atomic Instrument Company Model 510) which drove two scale of 64 Atomic Instrument Company Model 101-M scalers in series. A channel width of 2.0 volts was used throughout the experiment, although slightly more accurate results might have been obtained if this width had been adjusted for each of the amplifier gain settings used. Since the gain of the photomultiplier tube is a critical function of the tube voltage, (Breitenberger[39] reports that the photomultiplier tube gain varies as the 5.5 power of the voltage for a tube of 10 stages) a "Super-stable" high voltage power supply was used (Atomic Instrument Company Model 312).

The linearity of the pulse height scale was checked with a precision pulser Model 47, Mark 15, manufactured by Radiation Counter Laboratory. It was found that the scale was linear between 0 and 800 units, based on 1000 pulse height units full scale. Consequently, the gain was adjusted whenever possible so that all spectra were located between 0 and 800 pulse height units.

---

[39] Breitenberger, E., op. cit., (footnote 32).

In order to obtain the best resolution from the spectrometer, the optimum high voltage for the photomultiplier was obtained experimentally. The width of the cesium^{137} 32 Kev isotopic X-ray peak was used to determine the resolution at various photomultiplier voltages. In all cases the peak pulse height was adjusted by varying the coarse and fine gains so that the 32 Kev X-ray peak was at approximately 450 pulse height units. It was found that 730 volts produced the best resolution, and this voltage was therefore used throughout the experiment.

The preliminary calibration of energy versus pulse height was made using three isotopes produced in the Oak Ridge Graphite Reactor. These isotopes were selected on the basis that their gamma rays were in the energy range where the X-ray spectra were to be determined. Four isotopes were originally selected, but the fourth, osmium^{191}, presented such an unusual spectrum that it was not used in the original calibration. The isotope decay schemes are shown in Figure 3. These isotopes, originally in liquid form, were evaporated in glass ampoules 0.5 cm in diameter by 3 cm long and then sealed to prevent contamination. The original activity of the samples was about 2 millicuries except in the case of the shorter-lived osmium^{191} which was 4 millicuries in strength. Isotope spectra were obtained with the ampoules suspended approximately 20 cm above the scintillation crystal, and with a 0.9 cm Lucite plastic sheet over the crystal to attenuate the beta activity of the sample. The isotope spectra are shown in Figures 4, 5, 6 and 7.

UNCLASSIFIED
ORNL-LR-DWG. 29752

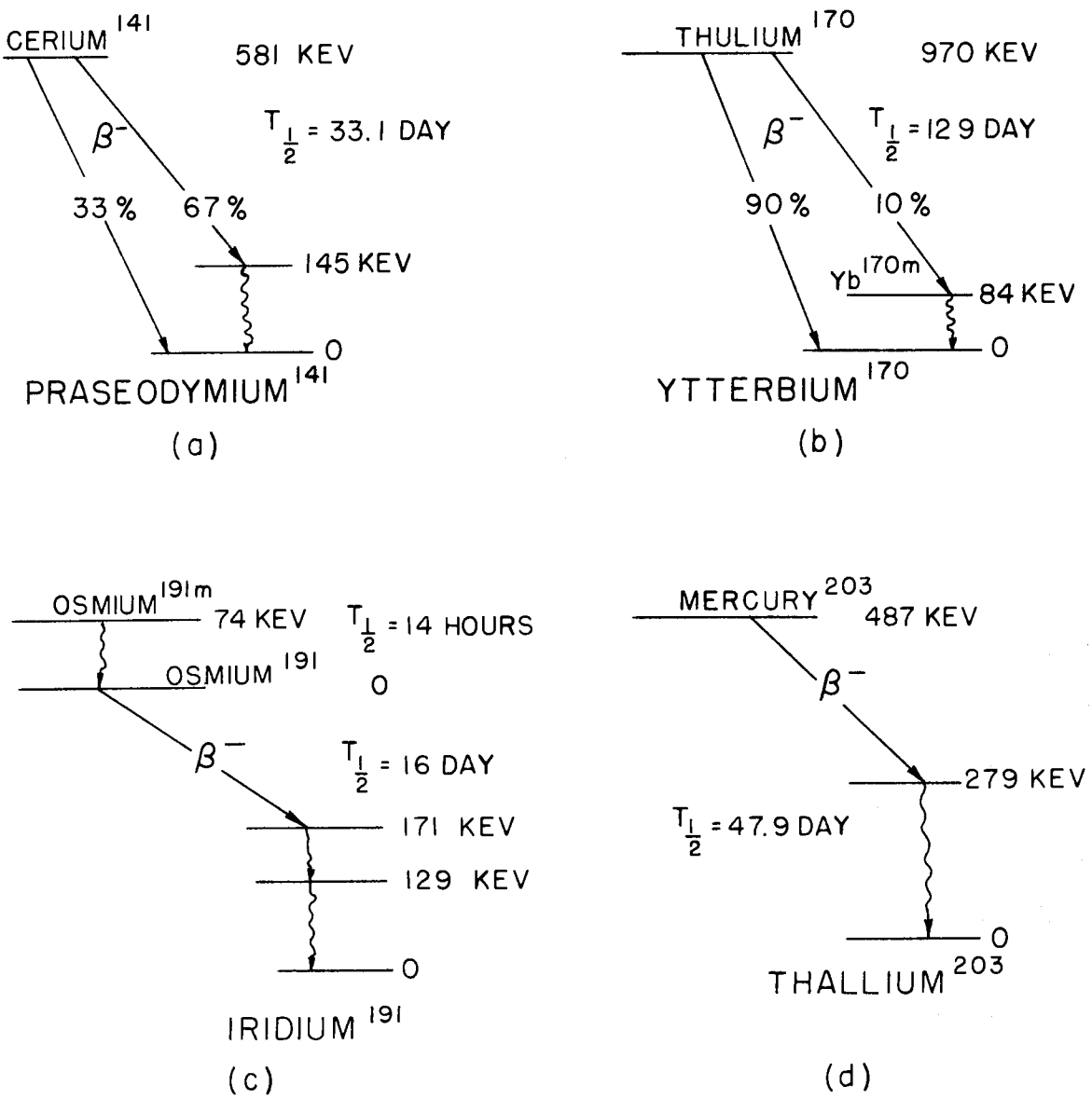

Figure 3. Isotope Decay Schemes, a) Cerium^{141}, b) Thulium^{170}, c) Osmium^{191}, d) Mercury^{203}.

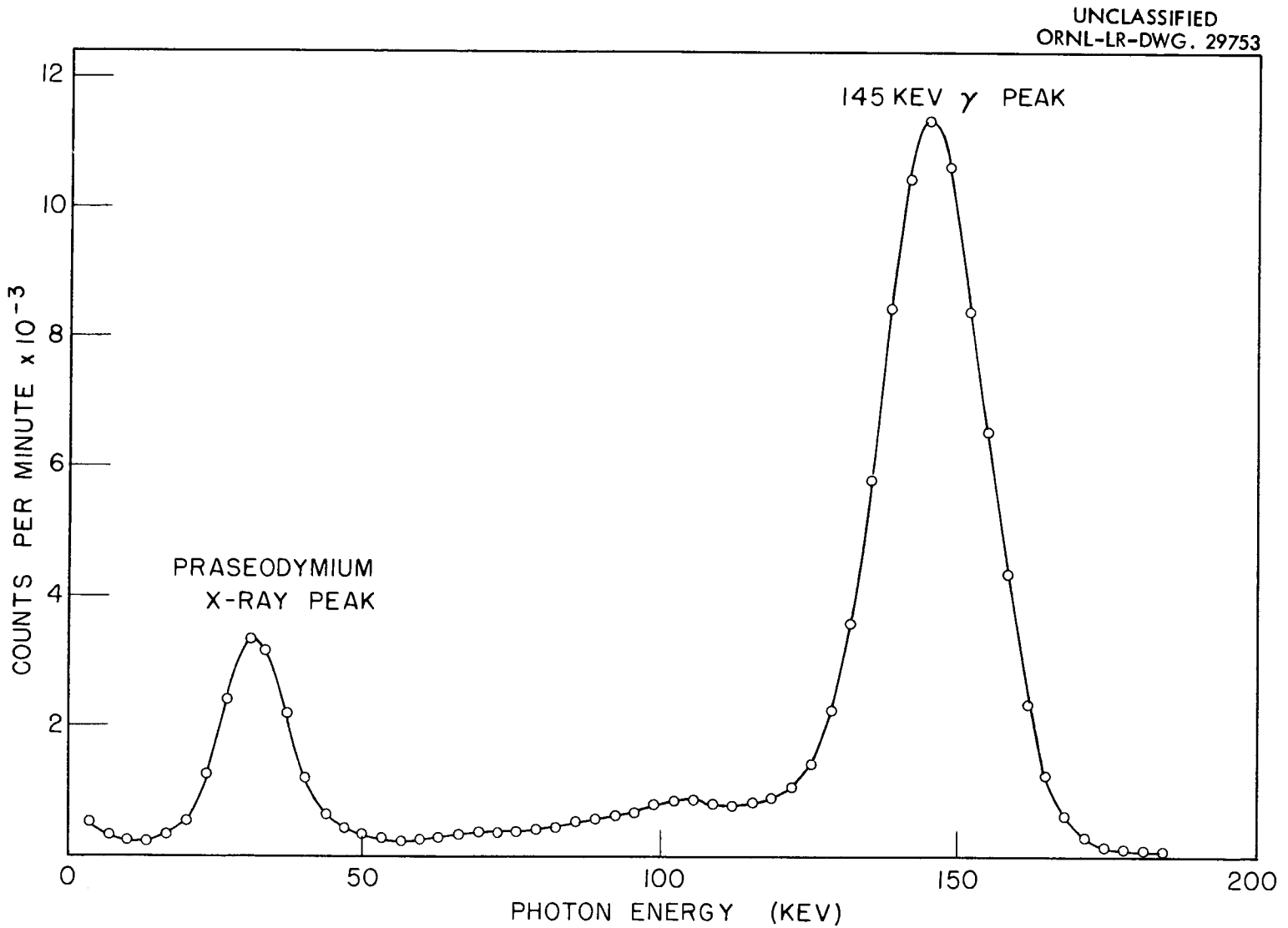

Figure 4. Cerium^{141} Spectrum.

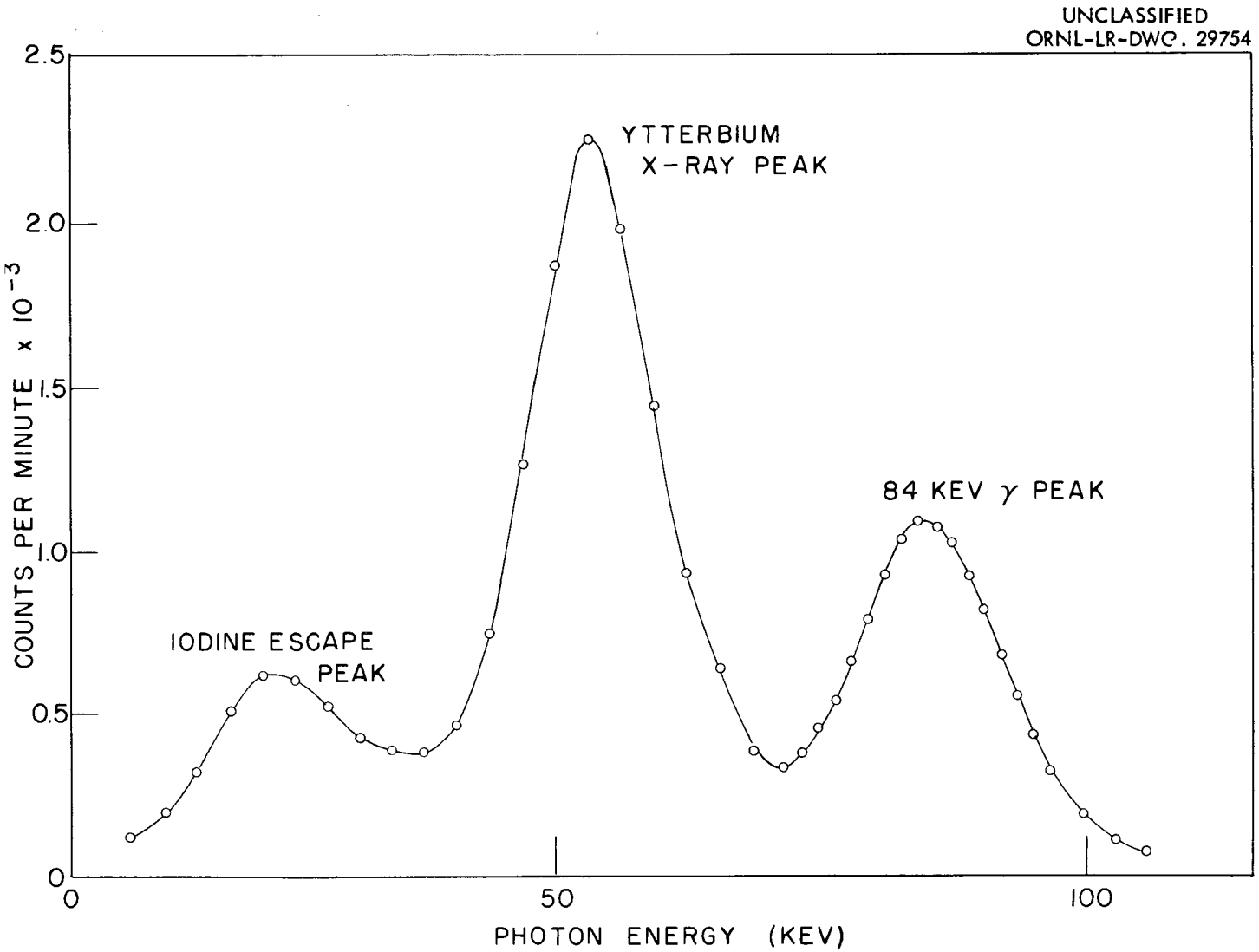

Figure 5. Thulium^{170} Spectrum.

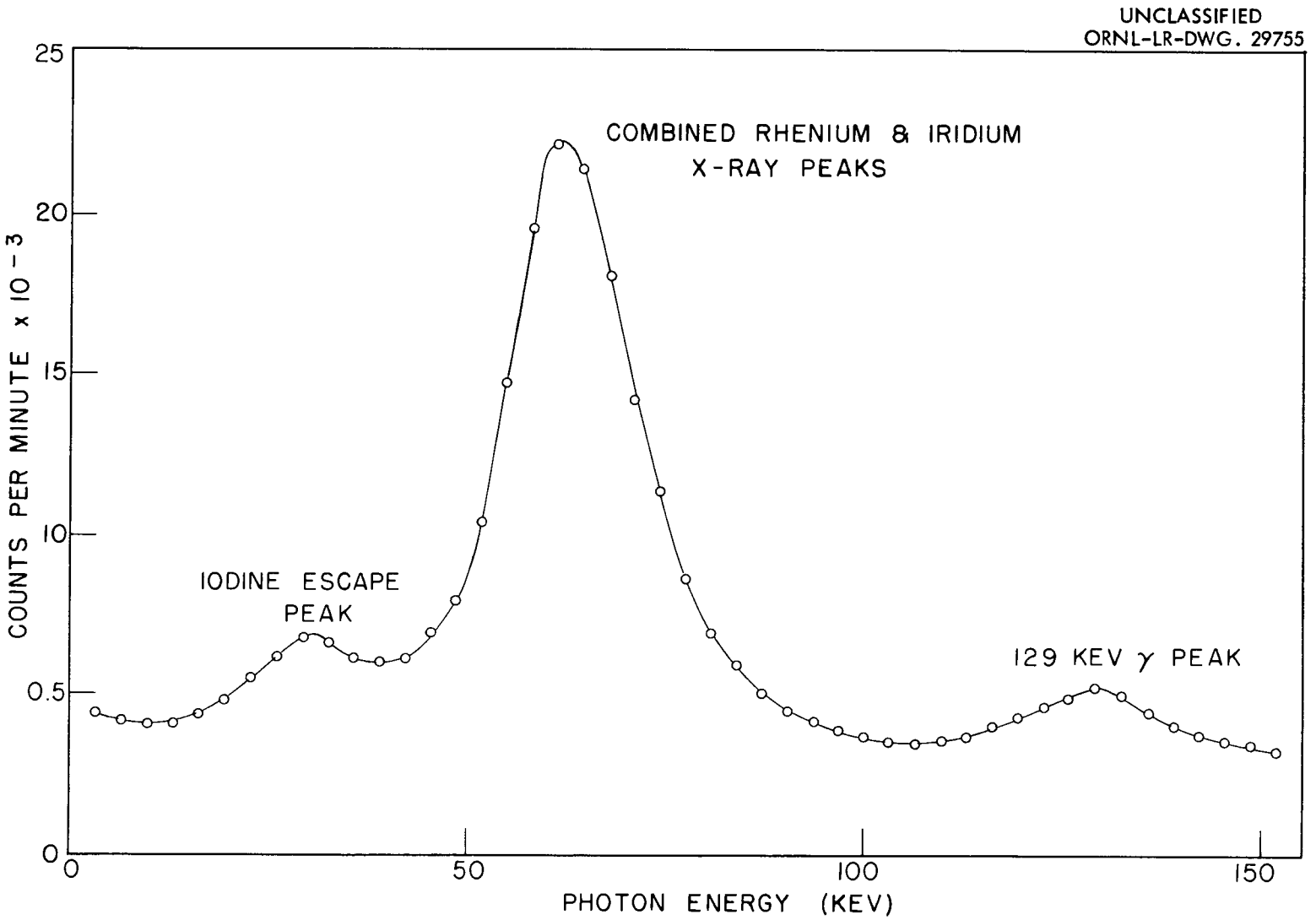

Figure 6. Osmium^{191} Spectrum.

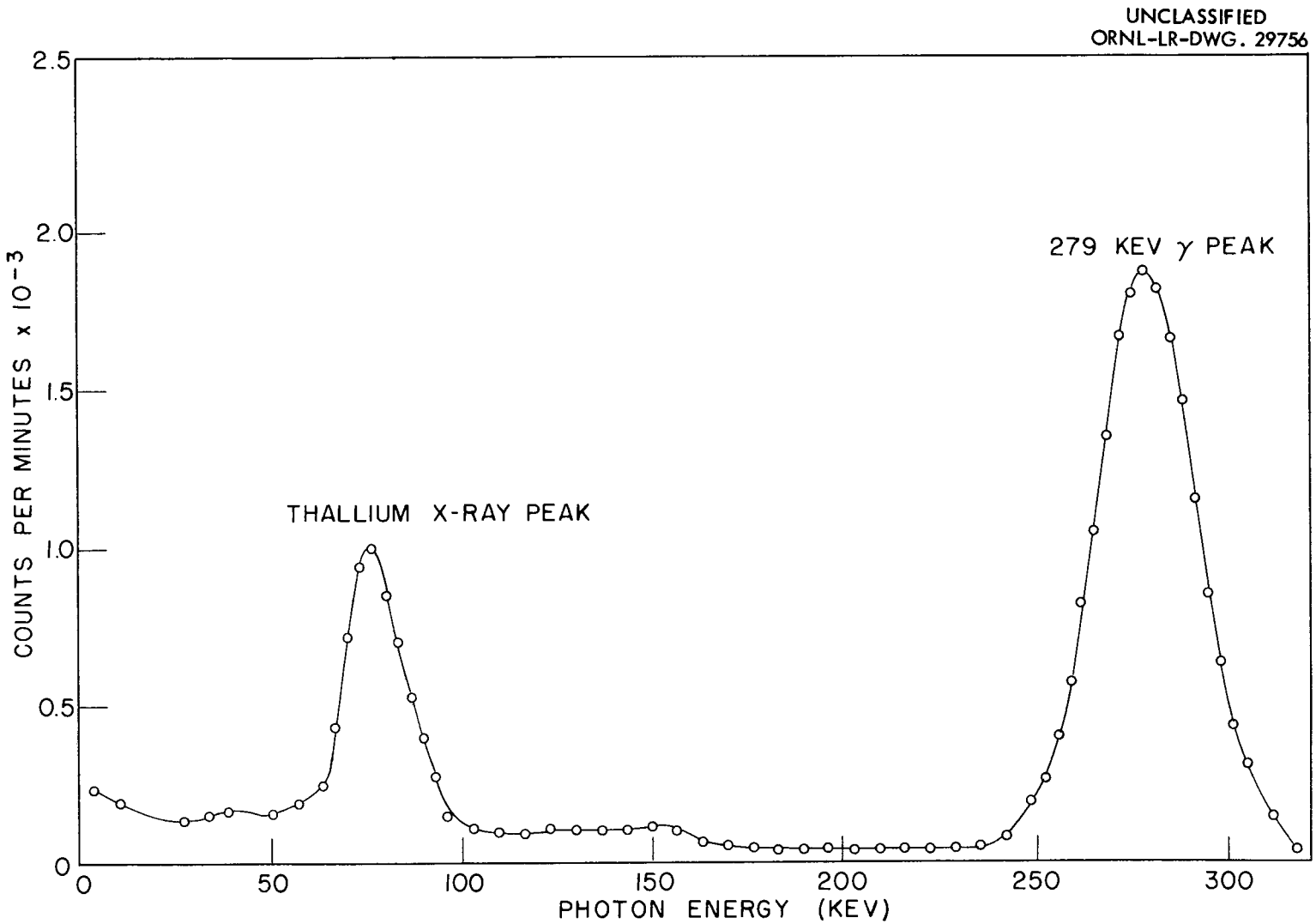

Figure 7. Mercury^{203} Spectrum.

The energy of the gamma rays was obtained from Seaborg[40] and the peak pulse height that corresponded to this energy was obtained by extrapolating the sides of the complete absorption peak to a point of intersection. A preliminary energy versus pulse height unit plot was made (Figure 8) so that the resolution curve could be plotted against energy (a more useful form) instead of against pulse height.

To obtain the preliminary data on the resolution as a function of energy, it was necessary to find the value of "a" for each of the isotope gamma peaks. The value of "a" can be found from Equation (3) in the following manner. If one takes the logarithm to the base 10 of both sides of the equation, the result is

$$\log_{10} G(h,H) = \log_{10} \frac{\alpha}{a\sqrt{\pi}} - \left[\frac{\alpha^2}{a^2} \log_{10} e \right] (h-H)^2 \qquad (5)$$

If the logarithm of the count rate, $G(h,H)$ is plotted versus $(h-H)^2 \equiv \Delta H^2$, the points should lie on a straight line with slope $\left[- \frac{\alpha^2}{a^2} \log_{10} e \right]$, provided the peak can be represented by a Gaussian. The quantity a^2 may be obtained then from

$$a^2 = - \frac{\alpha^2 \log_{10} e}{\text{slope}} \qquad (6)$$

---

40 Hollander, J. M., Perlman, I., and Seaborg, G. T., Revs. Modern Phys., 25, 613 (1953).

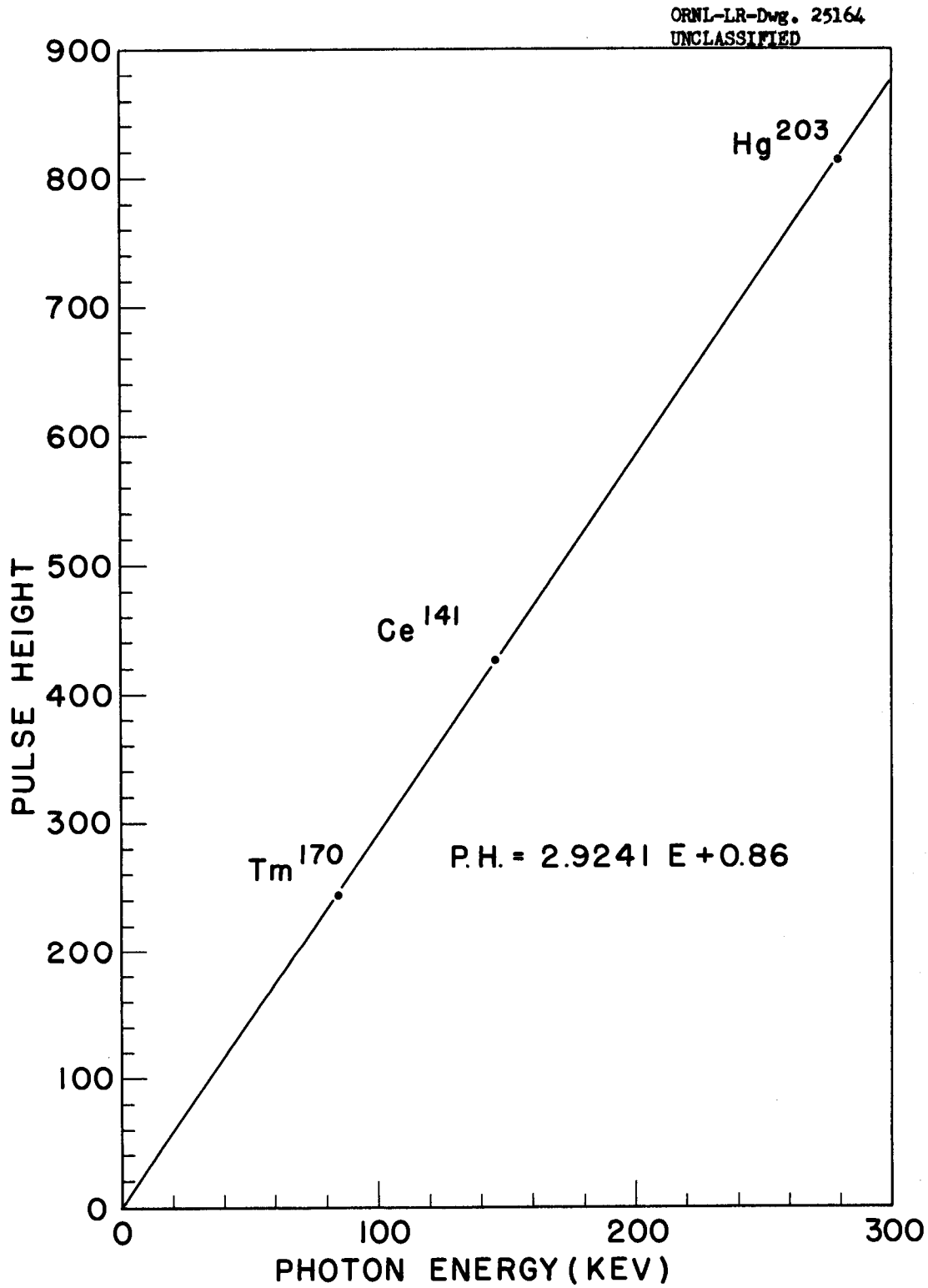

Figure 8. Pulse Height as a Function of Gamma Ray Energy.

As an alternative to taking the logarithm of the count rate, the count rate may be plotted on semi-logarithmic graph paper. Figure 9 is an example of this plot for the cerium^{141} gamma peak. This plot illustrates that the data follows a normal Gaussian distribution except for the base of the curve (large values of $(\Delta H)^2$). The cerium^{141} spectrum (Figure 4) shows that the base of the gamma peak on the low energy side is distorted due to the influence of iodine escape peak, which makes the counting rate actually higher than it should be. The values of a^2 obtained from Equation 6 are plotted in Figure 10 and the Equation of the line is fitted by the method of least squares. A comparison of the Gaussian distribution obtained from the a^2 values based on this least squares fit and the experimental distribution is shown in Figure 11. This figure also illustrates how the widths of the distributions increase as the energy increases.

It was apparent that more calibration points should be used, and thus that the information in Figures 8 and 10 should be regarded as preliminary. An inspection of other isotopes readily available indicated that another source of monoenergetic radiation should be obtained. (Most of the available low energy gamma emitters had complex spectra.) It was observed that the characteristic X-ray peaks produced when an isotope decays, could be used for calibration purposes. Characteristic X-rays are also produced when elemental materials are bombarded with X-rays of energy greater than the binding energy of the K-shell electrons. These fluorescent K X-rays are no different

ORNL-LR-Dwg. 25160
UNCLASSIFIED

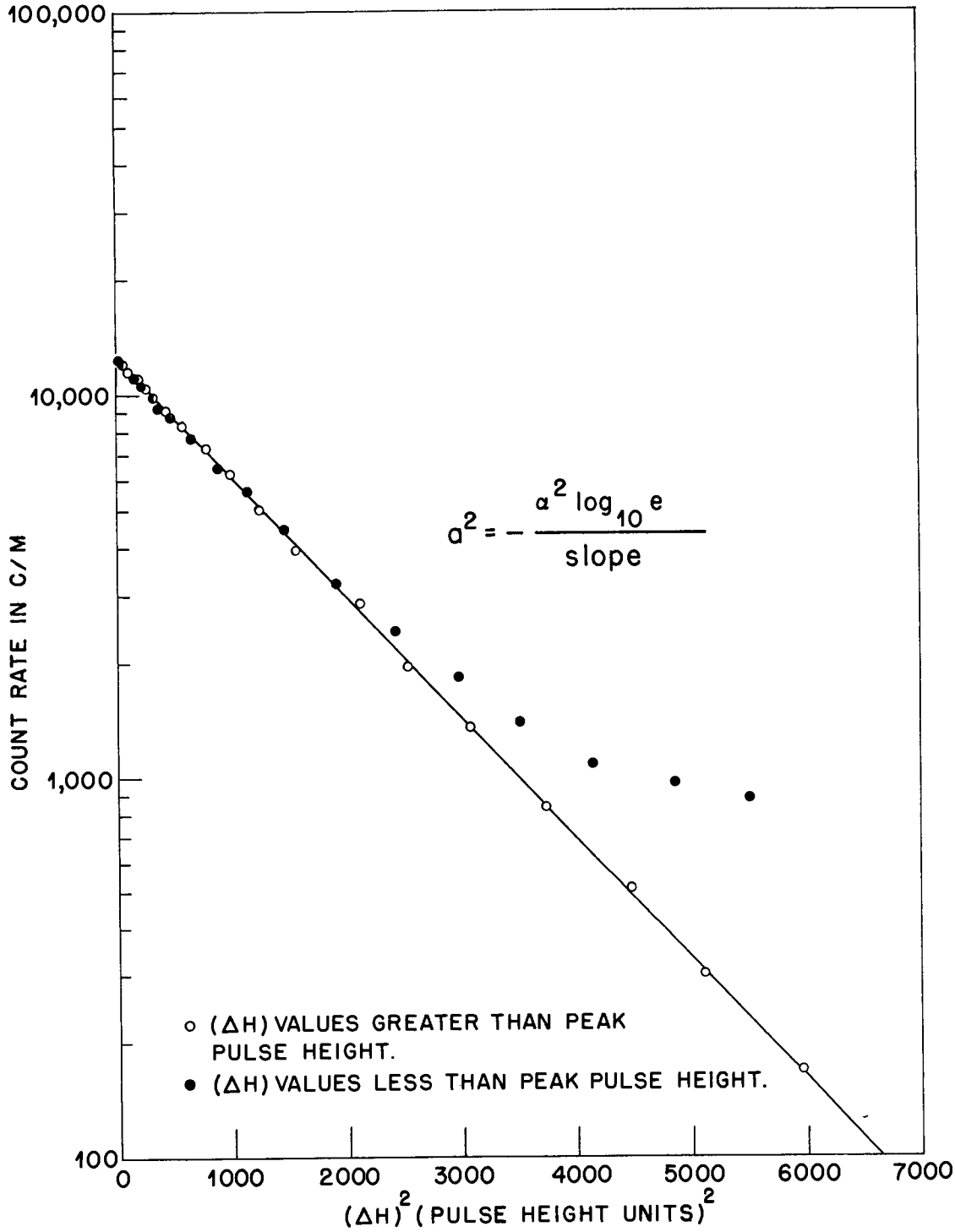

Figure 9. Gaussian Representation of Data, 145 Kev Cerium^{145} Gamma Peak.

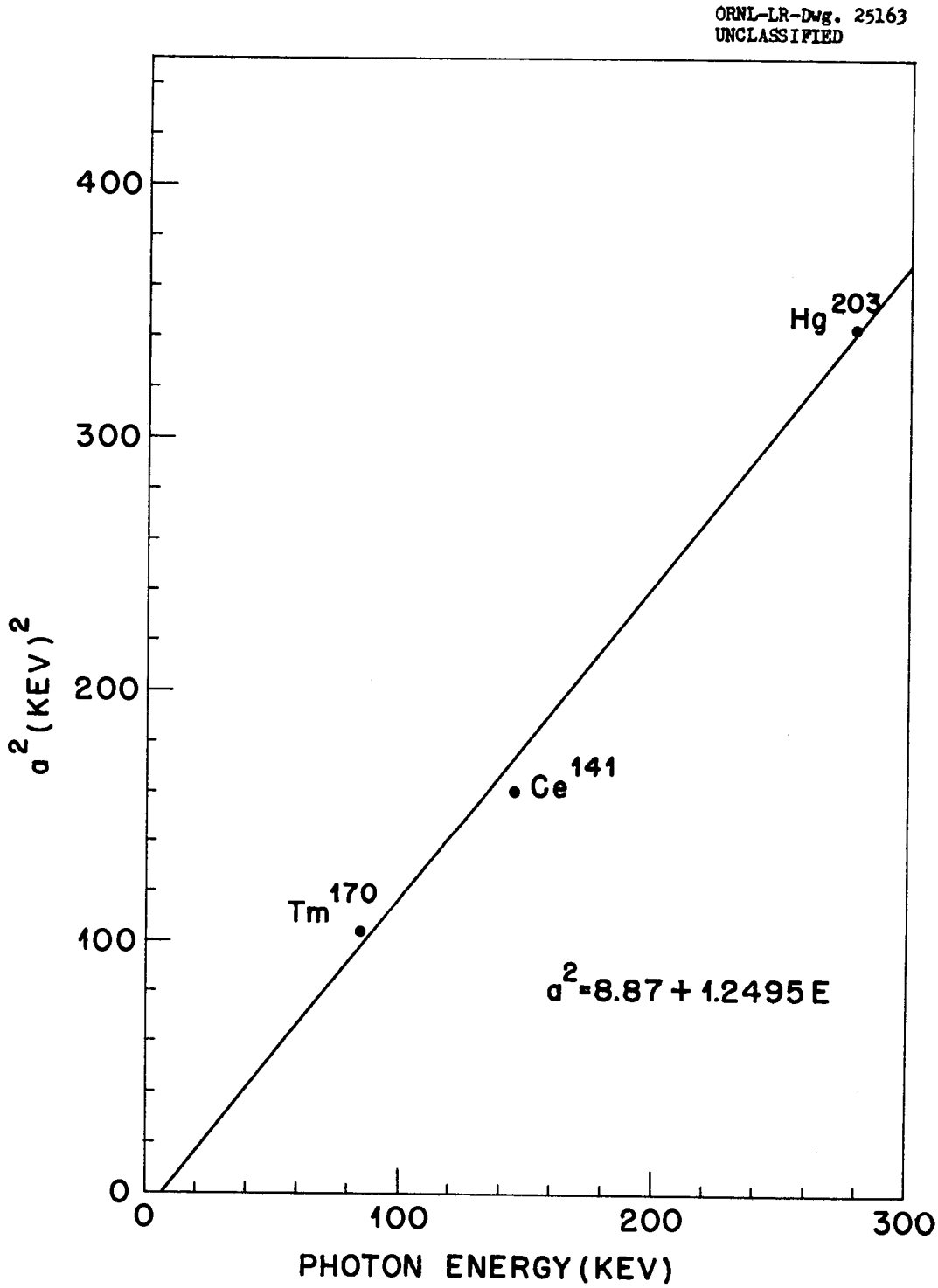

Figure 10. a^2 as a Function of Gamma Ray Energy.

ORNL-LR-Dwg. 25159
UNCLASSIFIED

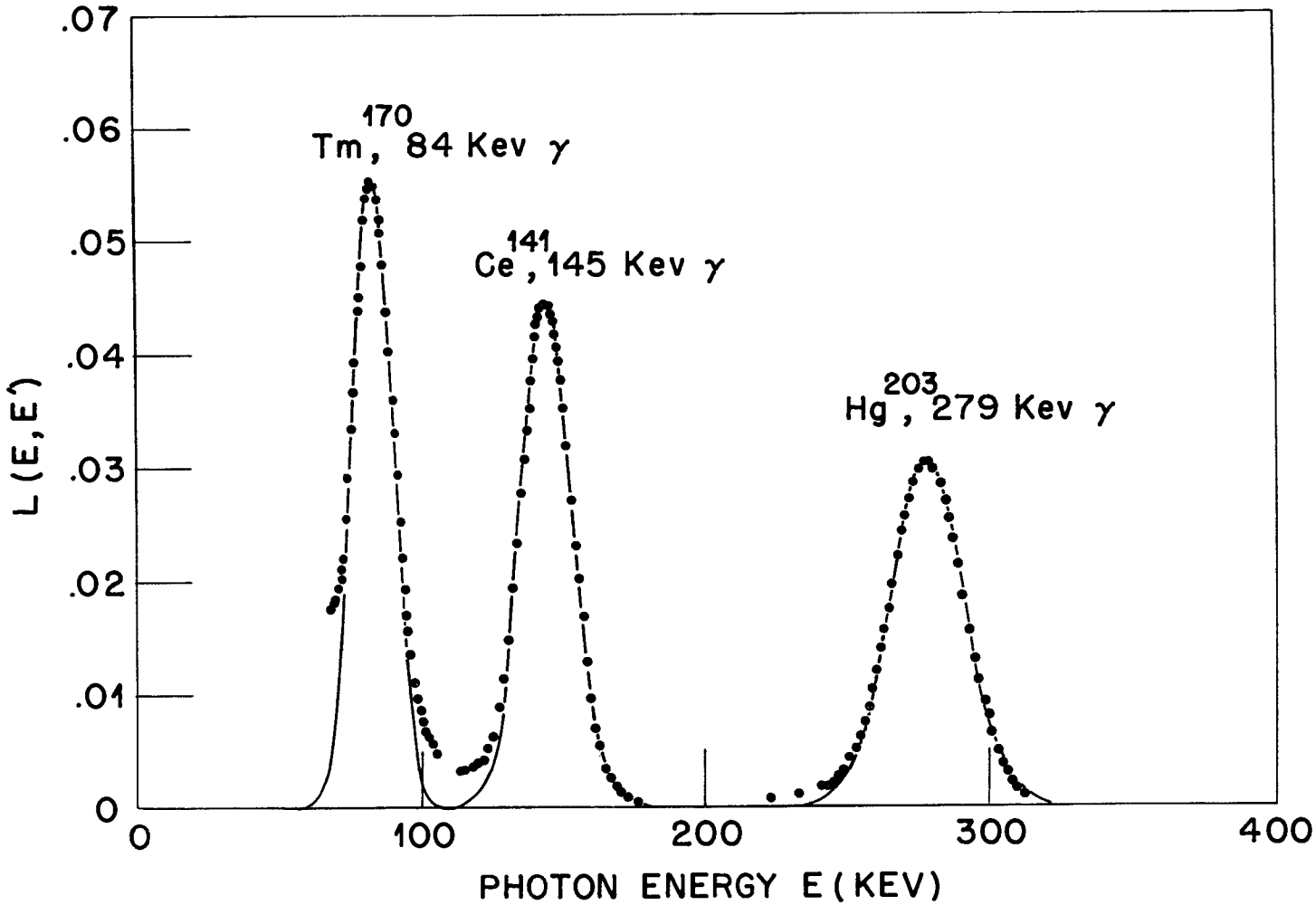

Figure 11. Comparison of Experimental Data (Dots) with Normalized Gaussian Curves (Lines).

in structure or origin than the K X-rays of isotopic decay. Either set of these K X-rays is made up of a fine structure of four basic monoenergetic K X-rays of known intensity and energy. They may be classed in order of their decreasing intensity as K_{α_1}, K_{α_2}, K_{β_1}, K_{β_2}. The energy range for these lines, varying from the lowest to highest, is K_{α_2}, K_{α_1}, K_{β_1}, and K_{β_2}. The actual intensity and energy of each set depends upon the atomic number of the element and the relative intensity of any line compared to the others in its set is also a function of the atomic number of the radiating material. Since each of these individual lines is monoenergetic, it will have a Gaussian distribution that should fit the same equation as the monoenergetic gammas. The energy difference between the lines in the K series is small; therefore, they cannot be separated by the scintillation spectrometer. Consequently, the spectrometer "sees" one distribution that is composed of all four of these lines and appears to be roughly a Gaussian of anomolous width. It is apparent that this distribution has a greater halfwidth at 1/e times the maximum and therefore a different a^2 value. This a^2 value will be greater than an a^2 value for a monoenergetic line with a corresponding energy, and will, therefore, fall above the equation of the line as plotted in Figure 10. This difference in resolution becomes striking when one examines the theoretical distributions of the K X-ray peaks for platinum as shown in Figure 12. These values are based on the

resolution curve obtained from the three isotopic gamma energies, with the energy and relative intensity values for platinum taken from the tables of Fine and Hendee[41] and Compton and Allison.[42] The intensity distribution recorded by the spectrometer would be the sum of the four individual K-series X-rays, represented as $\Sigma K_{\alpha+\beta}$. The curve will not only have a different a^2 value, but the energy of the peak will be different from any of the K_α or K_β energies. The peak energy values used throughout this experiment are obtained by extrapolating the sides of the distribution to a point of intersection.

In order to obtain a more precise estimate of the spectrometer resolution, it was felt that a correction curve should be made so that the a^2 values for the experimental K X-rays could be reduced to the a^2 value of a monoenergetic line. To do this, theoretical curves such as the example shown in Figure 12 were plotted for all the fluorescent and isotopic X-ray sources used in the experiment. The ratio of the a^2 value of the K_{α_1} distribution (the most intense line in the K series) to the a^2 value of the $\Sigma K_{\alpha+\beta}$ distribution was determined, and the results plotted against the energy of the K_{α_1} line as shown in Figure 13. This ratio when multiplied by the a^2 value determined from the experimental data, will result in an a^2 value that is equivalent to that of a monoenergetic gamma. It is noted in Figure 13 that the correction factor is greater at the higher energies (higher atomic number) because

---

41 Fine, S., and Hendee, C. F., Nucleonics, 13, No. 3, p. 36 (March, 1955).

42 Compton, A. H., and Allison, S. K., X-RAYS IN THEORY AND EXPERIMENT, (D. Van Nostrand Co., Inc., New York, 1935) pp. 637-646.

UNCLASSIFIED
ORNL-LR-DWG. 28569

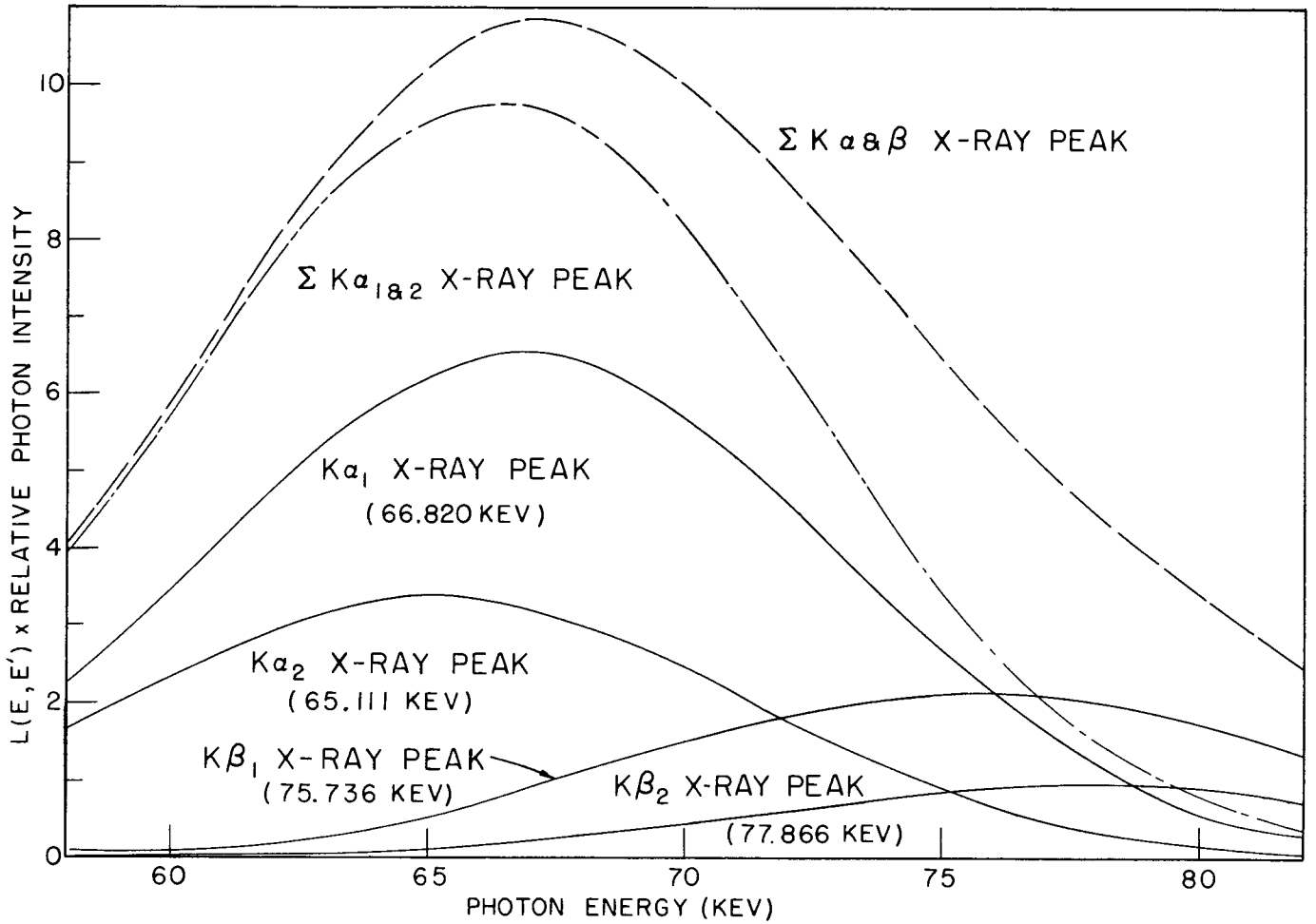

Figure 12. Change in Resolution of the Platinum K X-ray Spectra as a Result of K_β Contribution Based on $a^2 = 8.87 + 1.2495\ E$.

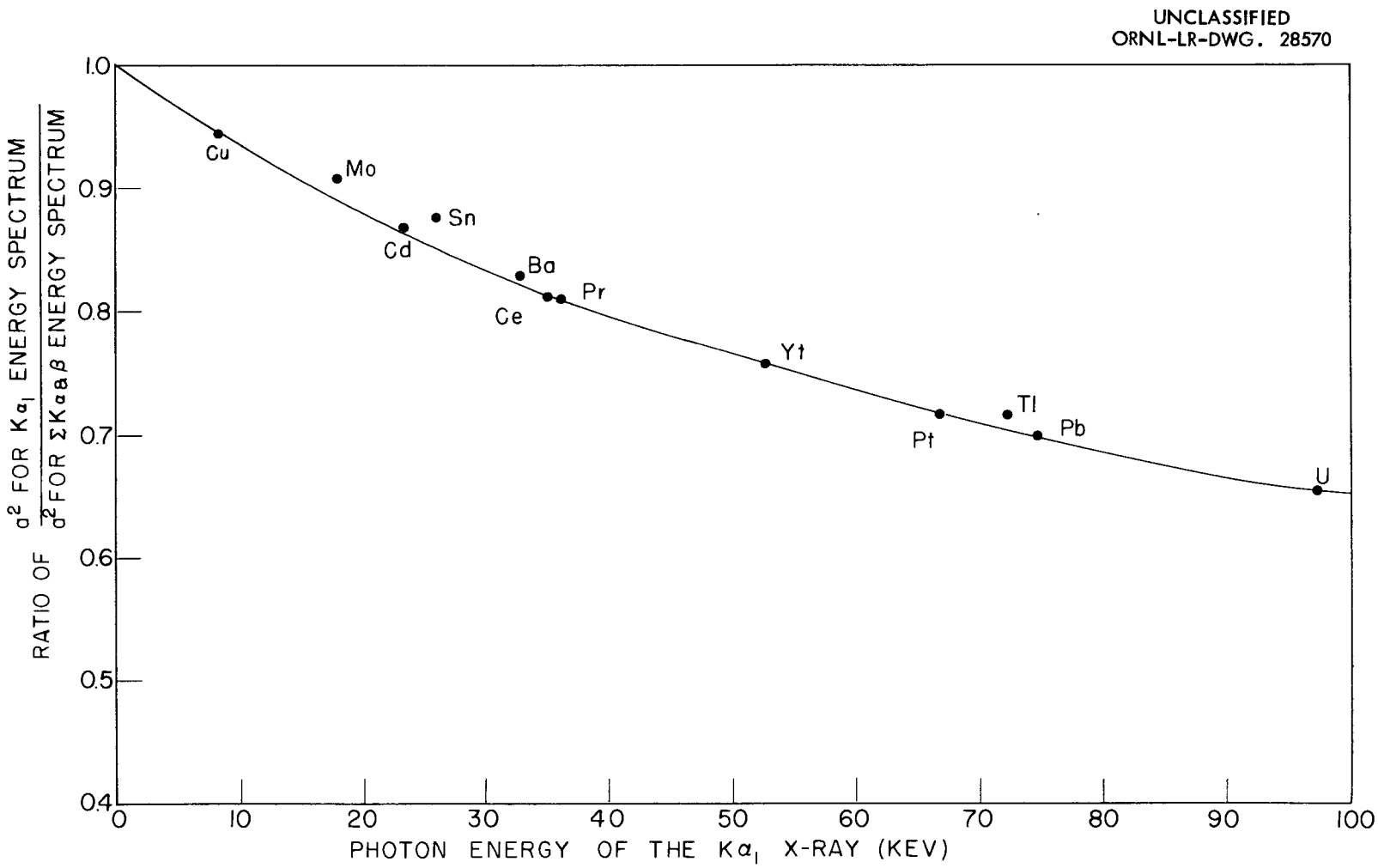

Figure 13. Resolution Correction Factors for the Experimental K X-ray Resolutions Based on $a^2 = 8.87 + 1.2495\ E$.

the energy spread of the K-lines increases with atomic number thereby increasing the width of the $\Sigma K_{\alpha+\beta}$ distribution.

Figure 12 indicates that the "envelope" resulting from the sum of the K_{α_1} and K_{α_2} lines is much narrower than the $\Sigma K_{\alpha+\beta}$ envelope. This is due to the relatively close spacing of the K_{α_1} and K_{α_2} lines. A correction factor (ratio of K_{α_1} to $\Sigma K_{\alpha_{1+2}}$) was also obtained for these values, but was found to be negligibly small, 0.93 for uranium, and 0.99 for lead. It was concluded that if the $K_{\beta_{1+2}}$ lines could be removed or filtered to a low intensity, the correction factor applied to the experimental resolution would be so small that it could be neglected, and the distribution could be treated as monoenergetic. It is, of course, impossible to remove complete the $K_{\beta_{1+2}}$ lines, but as pointed out by Seemann,[43] the proper choice of a filtering element with the proper thickness could reduce the $K_{\beta_{1+2}}$ to insignificant intensity. This filtering technique was used for the fluorescent X-rays, but the intensity of the isotopic X-rays was low and any additional filtration would have resulted in poor counting statistics. Consequently, the resolution correction curve was used for all the isotopic K X-rays.

The filtering element was chosen depending on the position of the K absorption edge of that particular material. As shown in Figure 1, there is a discontinuity in the absorption cross section which occurs at an energy equivalent to the binding energy of the K shell. If the

---

[42] Seemann, H. E., Rev. of Sci. Instr. 21, 314 (1950).

filtering element is chosen so the K edge energy falls between the energies of the K_{α_1} and K_{β_1}, then there will be a greater attenuation in the energy just above the K edge than just below it. This will result in greater absorption for the K_{β_1} and K_{β_2} energies than for the closely spaced K_{α_1} and K_{α_2}. The thickness of the filtering element was so selected in this experiment as to reduce the K_β components to 1/10 of their original counting rate. The absorption coefficients for most elements are available in the literature.[44,45] The experimental results for a filter with thickness chosen in accordance with the above are shown in Figure 14 for a uranium radiator. The improperly chosen tin filter does not change the resolution of the K X-ray peak because the K edge for tin is too low. It does, however, attenuate some of the low energy scatter radiation from the X-ray tube. Thorium is the proper filtering element and does decrease the width of the peak as is shown in Figure 15. Experimentally, the ratio of the resolution parameter a^2 for the uranium $K_{\alpha_1+\alpha_2+0.1\beta}$ obtained with the thorium filter to the a^2 for the unfiltered K series is 0.64 or compared with the calculated value of 0.69. The ratio of the calculated a^2 values for monoenergetic K_{α_1} to $K_{\alpha_1+\alpha_2+0.1\beta}$ is 0.94. It should also be noted that the thorium filter has reduced the counting rate to about 16 per cent of the original.

---

[44] Grodstein, F. W., Natl. Bur. of Standards Circular 583, (1957).

[45] Victoreen, J. A., J. Appl. Phys., 20, 1141 (1949).

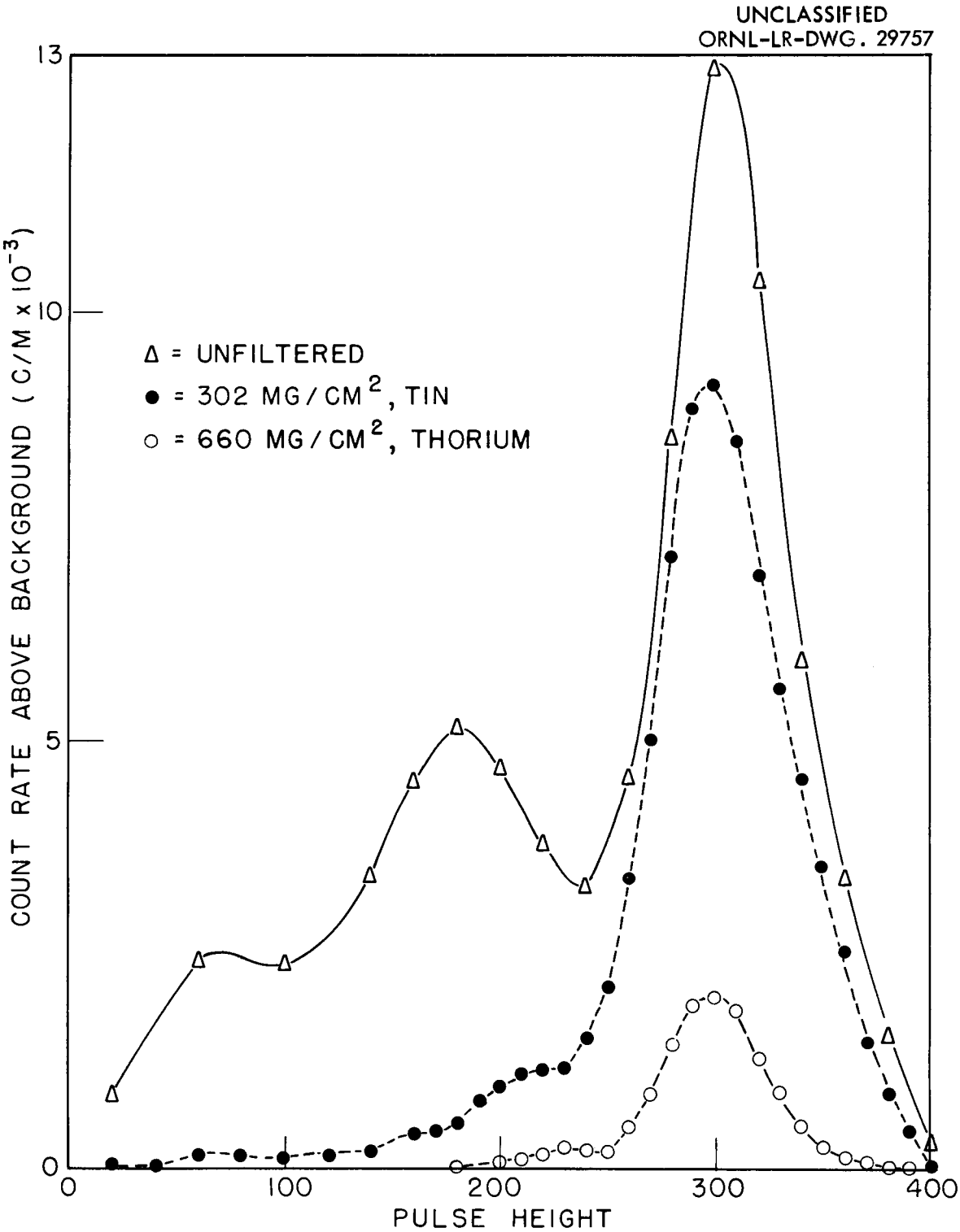

Figure 14. Comparison of Filtered and Unfiltered Fluorescent K X-ray Spectra of Uranium.

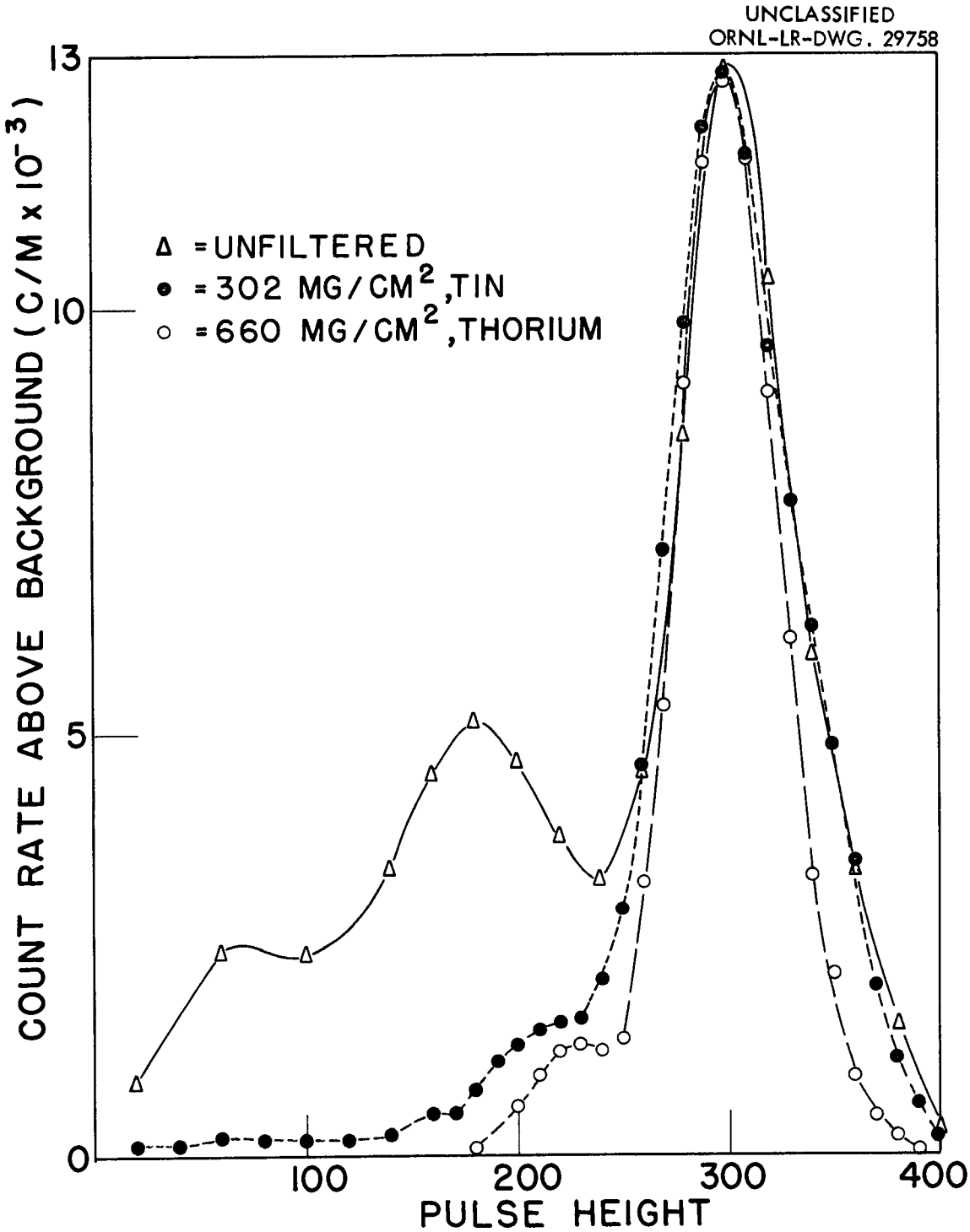

Figure 15. Comparison of Filtered and Unfiltered Fluorescent K X-ray Spectra of Uranium. Curves are Normalized to the Same Peak Count Rate.

The selection of a material for a radiator depends on the energy desired and the availability of the radiator and filtering element. The maximum energy for K X-ray emission is 97.2 Kev obtained from uranium, assuming that the transuranic elements are not available. A list of the K-fluorescent materials used in the experiment is shown in Table I. Some of these elements are not readily available in metallic foil form; therefore, compounds were selected in which the predominant element was element desired, and the remaining elements were of low atomic number and would not produce interfering K X-rays. A method was devised to convert the compounds in powder form to a "foil". A predetermined weight of the compound, based on the weight of the element per 3 inch square filter to give the necessary attenuation, was mixed with a liquid plastic called "Castolite". After thorough mixing, a "hardener" was added to the liquid form, and the mixture was poured into a mold three inches square and 3/8 inches deep. After several hours, the plastic hardened into a solid block and could be taken from the mold. The block then had the necessary mass of filtering element per unit area for proper absorption. The primary advantages of this method of preparing filters is that the filters can be made into any thickness desired, and they can be stored in a safe form. The attenuation of the small amount of plastic used is negligible because of the low atomic number of the elements in the plastic.

The disadvantage of this procedure is that certain compounds, primarily nitrates, do not mix with the plastic. A method suggested

Table I. Fluorescent Radiators Used For Spectrometer Calibration

Element	K Series, Critical Emission Energies in Kev.*				Energy of the K Series Peak (Kev)≠	X-Ray Exciting Potential In Kev. (Tube Current=20MA)	Form of Radiator	Filtering Element	Form of Filter
	K_{β_2}	K_{β_1}	K_{α_1}	K_{α_2}					
Cu	8.976	8.904	8.047	8.027	8.07	50	Sheet	None	None
Mo	19.964	19.607	17.478	17.373	17.75	50	Sheet	None	None
Cd	26.641	26.093	23.172	22.982	23.36	50	Sheet	None	None
Sn	29.106	28.483	25.270	25.042	25.60	50	Sheet	None	None
Ba	37.255	36.376	32.191	31.815	32.65	50	$BaCO_3$	None	None
Ce	40.231	39.255	34.717	34.276	34.6**	50	$Ce(NO_3)_3 \cdot 6H_2O$	Barium	$BaCO_3$, ~100 MG/CM^2
Pt	77.866	75.736	66.820	65.111	66.2**	150	Sheet	Tungsten	Metallic Powder, ~280 MG/CM^2
Pb	87.343	34.922	74.957	72.794	74.2**	150	Sheet	Mercury	$Hg(NO_3)_2 \cdot H_2O$, ~ 400 MG/CM^2
U	114.549	111.289	98.428	94.648	97.2**	150	Sheet	Thorium	$Th(NO_3)_4 \cdot 12H_2O$ Solution, ~ 660 MG/CM^2

≠ Peak Energy Values determined by graphically extrapolating the slopes of the Gaussian energy distribution to a point of intersection.

* From: "X-Ray Critical - Absorption and Emission Energies in Kev" by S. Fine and C. F. Hendee, Nucleonics, 13, No. 3 (March, 1955).

** Only K_{α_1} and K_{α_2} lines used.

by Larson[46] was used, in which a predetermined weight of the compounds was heated to the melting point and then allowed to solidify into a mold of given area. These compounds were then coated with a protective coat of plastic, since some of the compounds were toxic. The thorium nitrate, because of the radiation hazard, was kept in solution in a plastic bottle. The depth of the solution was adjusted to correspond to the necessary thickness of thorium needed.

The techniques described above have the advantage of increasing the possibilities of the fluorescent X-ray method. If only metallic foils were used, the number of elements available in this form would be small; also, the exact thickness needed for proper attenuation might not be obtainable.

Figure 16 shows the schematic diagram of the fluorescent X-ray apparatus. The walls of the radiation chamber were made of sufficient thickness to prevent the scattered radiation from striking the scintillation crystal.

The additional K X-ray data obtained from both fluorescent radiation and isotopic decay enabled additional calibration points to be plotted together with the previous gamma ray data as shown in Figure 17 for values obtained on gain 2, 4 and 8 on the linear amplifier -- the gains used to take the X-ray spectra. The resolution of each of the peaks was determined in the manner previously illustrated in Figure 9. Appropriate corrections were applied to these a^2 values as described

---

46 Larson, H. V., Myers, I. T., and Roesch, W. C., HW-31781, Hanford Atomic Products Operation, Richland, Washington, (1954).

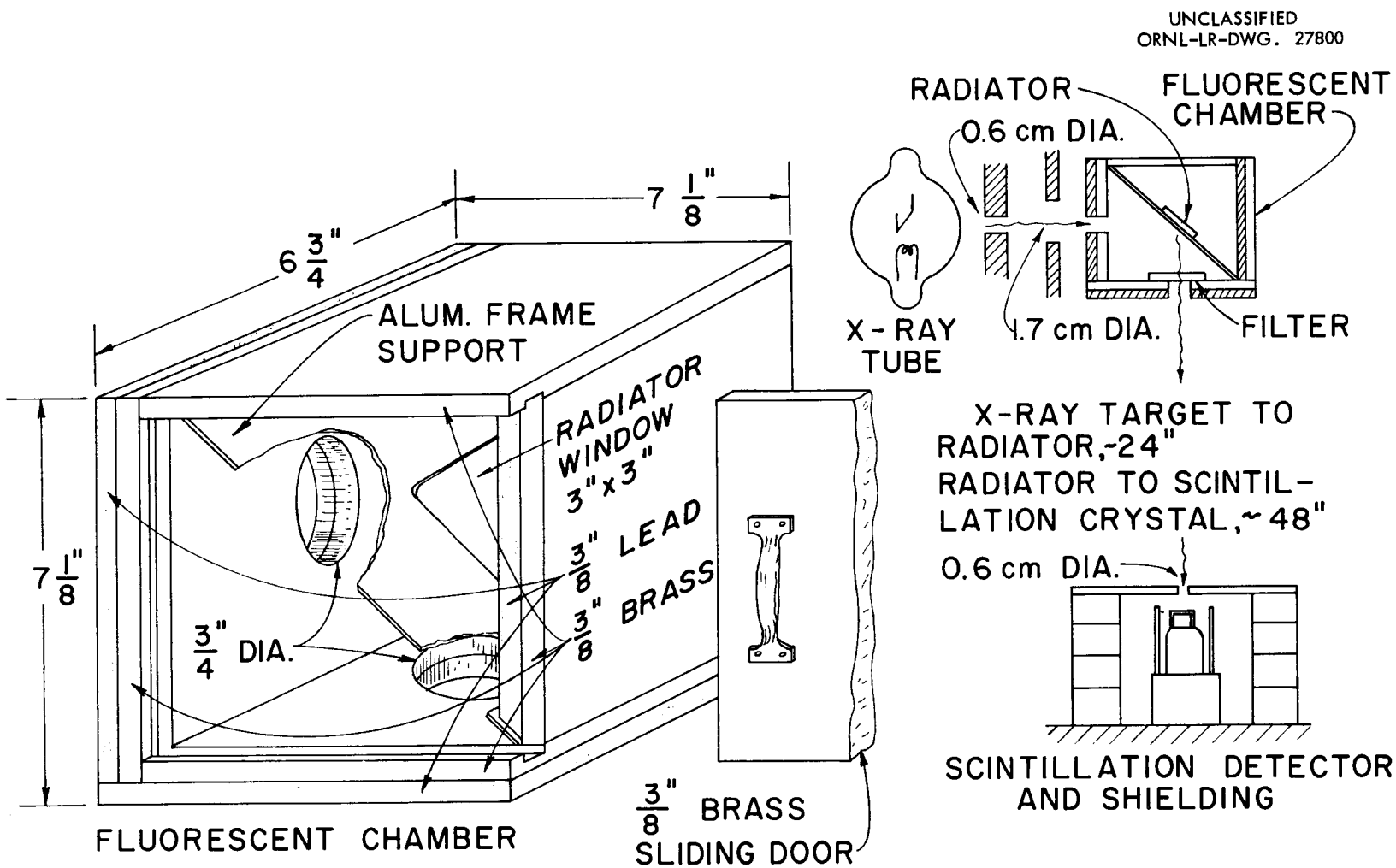

Figure 16. Schematic Diagram of the Fluorescent X-ray Apparatus.

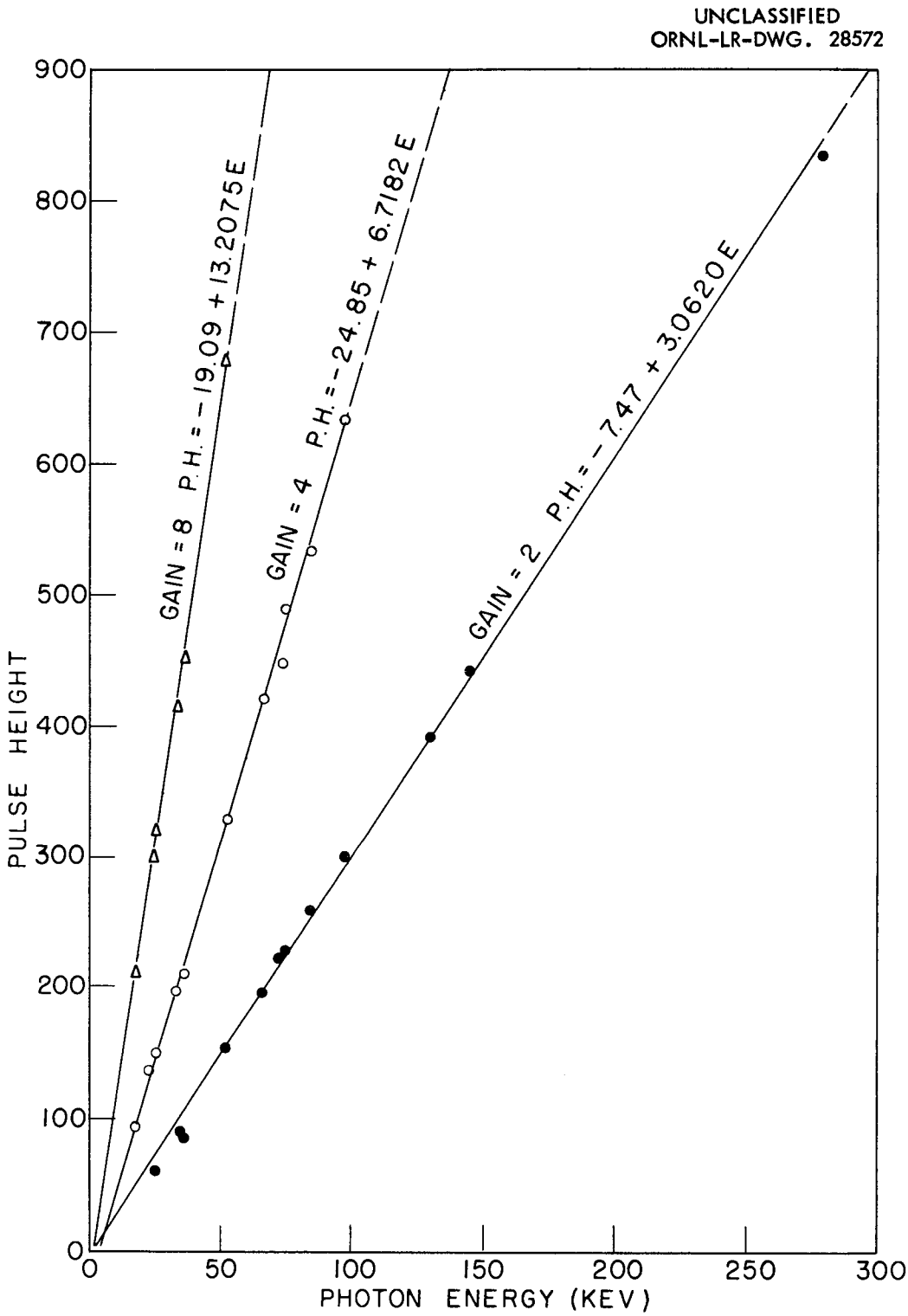

Figure 17. Pulse Height as a Function of Photon Energy.

earlier. This resulted in the final calibration plot, Figure 18, for the data obtained on gains 2, 4 and 8. The resolution differed from gain to gain because the channel width of the single channel pulse height analyzer was held constant at 2.0 volts throughout the experiment. If the channel width had been adjusted for each gain, the a^2 versus energy plot could have been represented by one line for all the gains. Unlike the preliminary calibration curve, Figure 10, the least square fit of the curve in Figure 18 was made to pass through the origin, since it was assumed that at zero energy, there should be zero resolution. The least square fit was checked for validity by the "t" test and found to be significant (Appendix A). The numbers attached to the curves in Figures 17 and 18 are estimated to be correct to within $\pm$ 2%. The additional digits were included to eliminate cumulative errors in computing with these values.

Table II is a complete list of all the sources used in calibrating the scintillation spectrometer for energy and resolution. It will be noted that in the final calibration the osmium^{191} gamma peak was used. Sufficient time elapsed after running the spectrum of osmium^{191} that all the peaks could be identified by their appropriate half-life. The tallest peak is the combination of the X-ray peaks from both the beta decay of osmium^{191} and the electron capture of osmium^{185}, a common contamination. This combined X-ray peak was not used because of its poor resolution.

After the scintillation spectrometer was calibrated, the necessary information was available to make possible appropriate corrections to the experimental X-ray spectra.

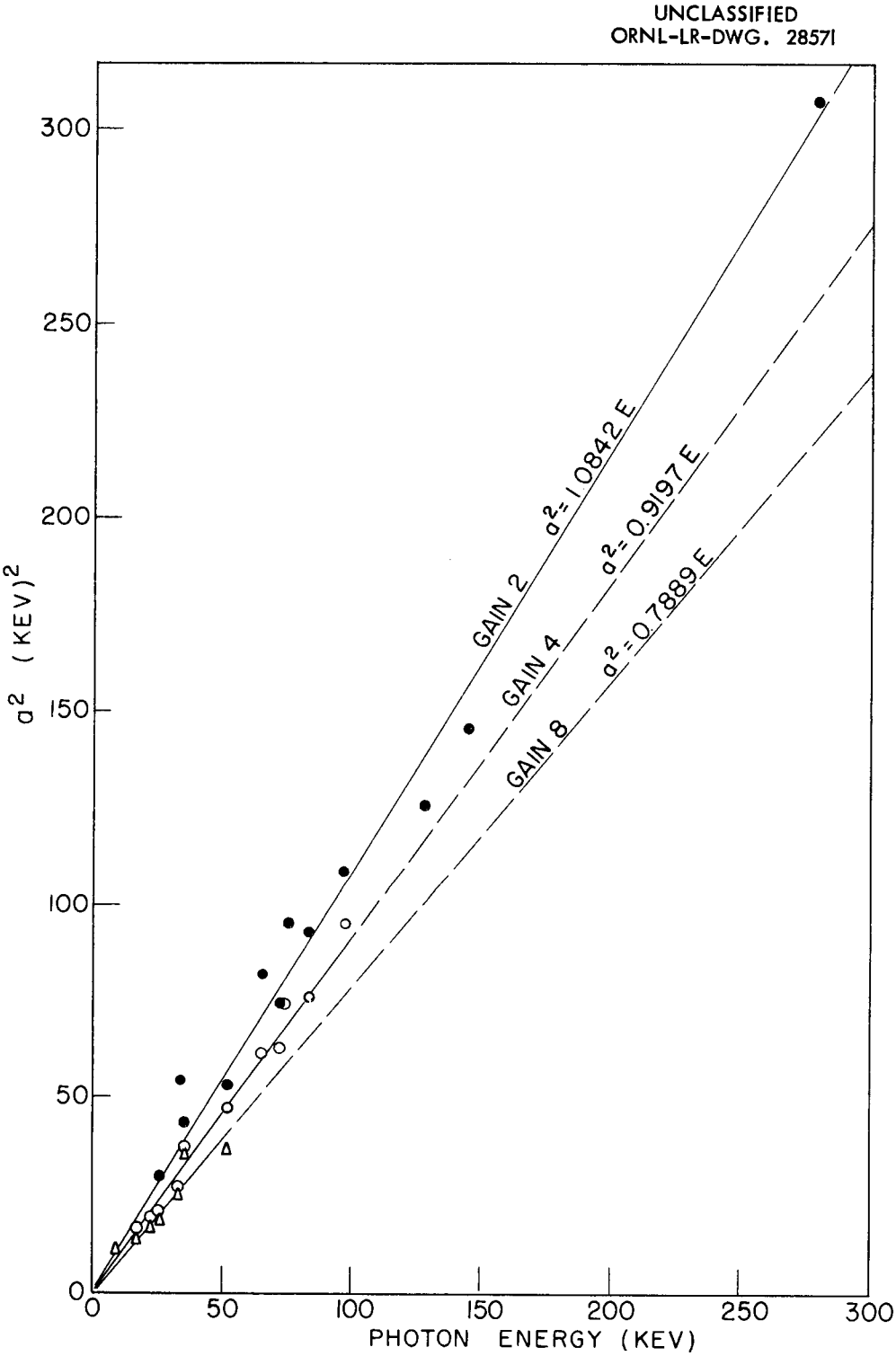

Figure 18. a^2 as a Function of Photon Energy.

Table II. Summary Data for Calibration

Source of Radiation	Method of Production	Photon Energy	Peak Value in Pulse Height Units			a^2 (Kev^2)		
			Gain 2	Gain 4	Gain 8	Gain 2	Gain 4	Gain 8
Cu	Fluorescent K X-ray	8.07	--	--	62	--	--	10.9
Mo	Fluorescent K X-ray	17.75	--	95	212	--	15.5	14.2
Cd	Fluorescent K X-ray	23.36	--	137	299	--	19.3	18.7
Sn	Fluorescent K X-ray	25.60	61	148	320	29.2	20.0	19.9
Ba	Fluorescent K X-ray	32.65	--	195	415	--	26.3	25.0
Ce	Fluorescent K X-ray *	34.6	90	--	--	54.9	--	--
Pr	Isotopic K X-ray	36.2	87	210	452	43.3	36.2	36.0
Yb	Isotopic K X-ray	52.6	153	329	679	52.6	46.0	36.1
Pt	Fluorescent K X-ray *	66.2	197	421	--	81.8	60.4	--
Tl	Isotopic K X-ray	72.3	223	448	--	73.7	62.4	--
Pb	Fluorescent K X-ray *	74.3	228	489	--	95.3	73.0	--
Tm	Gamma Decay of Tm^{170}	84.	257	533	--	92.2	74.6	--
U	Fluorescent K X-ray *	97.2	300	632	--	108.7	94.5	--
Os	Gamma Decay of Os^{191}	129	392	--	--	125.9	--	--
Ce	Gamma Decay of Ce^{141}	145	443	--	--	145.8	--	--
Hg	Gamma Decay of Hg^{203}	279	835	--	--	306.3	--	--

* Only the K_{α_1} and K_{α_2} X-rays used. (K_β Filtered)

V. CORRECTION OF THE X-RAY SPECTRA

The experimental arrangement used to obtain the X-ray spectra is shown in Figure 2. The X-ray machine was a commercial 250 Kv constant potential Westinghouse "Quandrocondex" unit operating with a 2% ripple. A Sorenson A.C. voltage regulator supplied a stable voltage to the X-ray transformer. Minor changes had been made on the X-ray machine. Additional lead shielding was placed over the X-ray tube housing to reduce the background level during the experiment. The actual X-ray tube voltage was indicated on two voltmeters which indicated respectively the filament potential below ground and the anode potential above ground. These meters were calibrated with a potentiometer and were found to be accurate with 1/2%.

Six experimental X-ray spectra were obtained using filtered primary beams. The filter elements and thicknesses were modifications of filters suggested by Ehrlich.[47] The components of the filters are listed in Table III, as well as the voltages and currents used. Low tube currents were used to prevent overloading of the spectrometer which would result in distortions at high counting rates.

A correction of the various distortions which influence the experimental spectra was accomplished in the reverse order from that in which these distortions occur. That is, the correction for the photomultiplier Gaussian resolution was carried out before the corrections were applied for the events which take place in the scintillation crystal.

---

[47] Ehrlich, M., and Fitch, S. H., Nucleonics, 9, No. 3, p. 5 (Sept. 1951).

Table III. Kilovolt Settings and Standard Filtration

Spectrum Desired (Kev)	Observed Voltage (Kev)	X-Ray Machine Dial Setting (Kev)	X-Ray Tube Current (Microamps)	Additional Filtration in $Mg/_{Cm^2}$*			
				Lead	Tin	Copper	Aluminum
250	251.8	238	40	2,363	861	959	279
200	199.5	188	20	716	1,863	929	279
150	148.1	138	30	---	913	2,790	279
100	98.7	92	12	548	---	---	279
50	49.5	44	20	---	---	233	133
30	29.6	18	40	---	---	---	133

* Inherent tube filtration equivalent to 661 $Mg/_{Cm^2}$ of Aluminum as determined from absorption curves with no added filtration, using data given by Taylor in "Physical Foundations of Radiology" by Glasser, O., Quimby, E. H., Taylor, L. S., and Weatherwax, J. L., (Paul B. Hoeber, Inc., New York, Second Edition, 1952) pp. 245-249.

As Freedman, et. al.,[48] pointed out, the measured spectrum $M(E)$ is related to the true spectrum $N(E)$ by the equation

$$M(E) = \int_0^\infty N(E')\, L(E,E')\, dE' \tag{7}$$

or, written as a summation

$$M(E) \simeq \sum_{i=0}^{\infty} N(E_i')\, L(E,E_i')\, \Delta E_i' \tag{8}$$

where $L(E,E_i')$ is the resolution of the spectrometer as obtained from equation (4), and is shown plotted in Figure 19.

In the iterative method of Freedman, the measured spectrum $M(E)$ is used in order to start the iterative procedure and a new spectrum $M_1(E)$ is generated.

$$M_1(E) = \sum_{i=0}^{\infty} M(E_i')\, L(E,E_i')\, \Delta E_i' \tag{9}$$

This new spectrum will in general be even more distorted by the Gaussian smearing function than the measured spectrum. The product of $M(E_i')\, L(E,E_i')$ is shown for the experimental 250 Kev X-ray spectrum in Figure 20. As a first approximation, the true spectrum $N_1(E)$ may be assumed to differ from $M(E)$ by the same amount that $M_1(E)$ differs from $M(E)$, but in an opposite direction, i.e., if

---

48 Freedman, M. S., Novey, T. B., Porter, F. T., and Wagner, F., op. cit. (footnote 38).

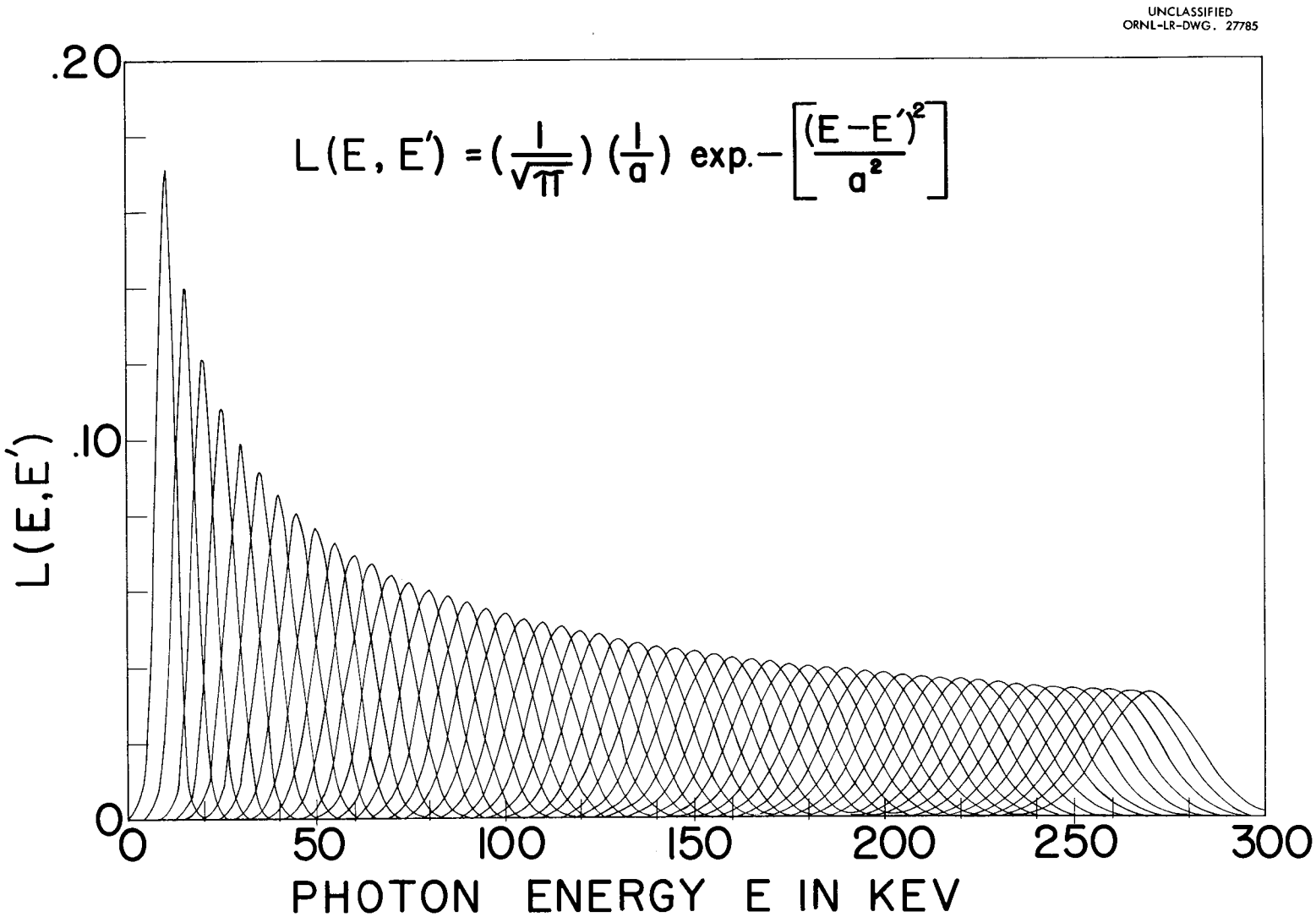

Figure 19. Normalized Gaussians.

UNCLASSIFIED
ORNL-LR-DWG. 27784

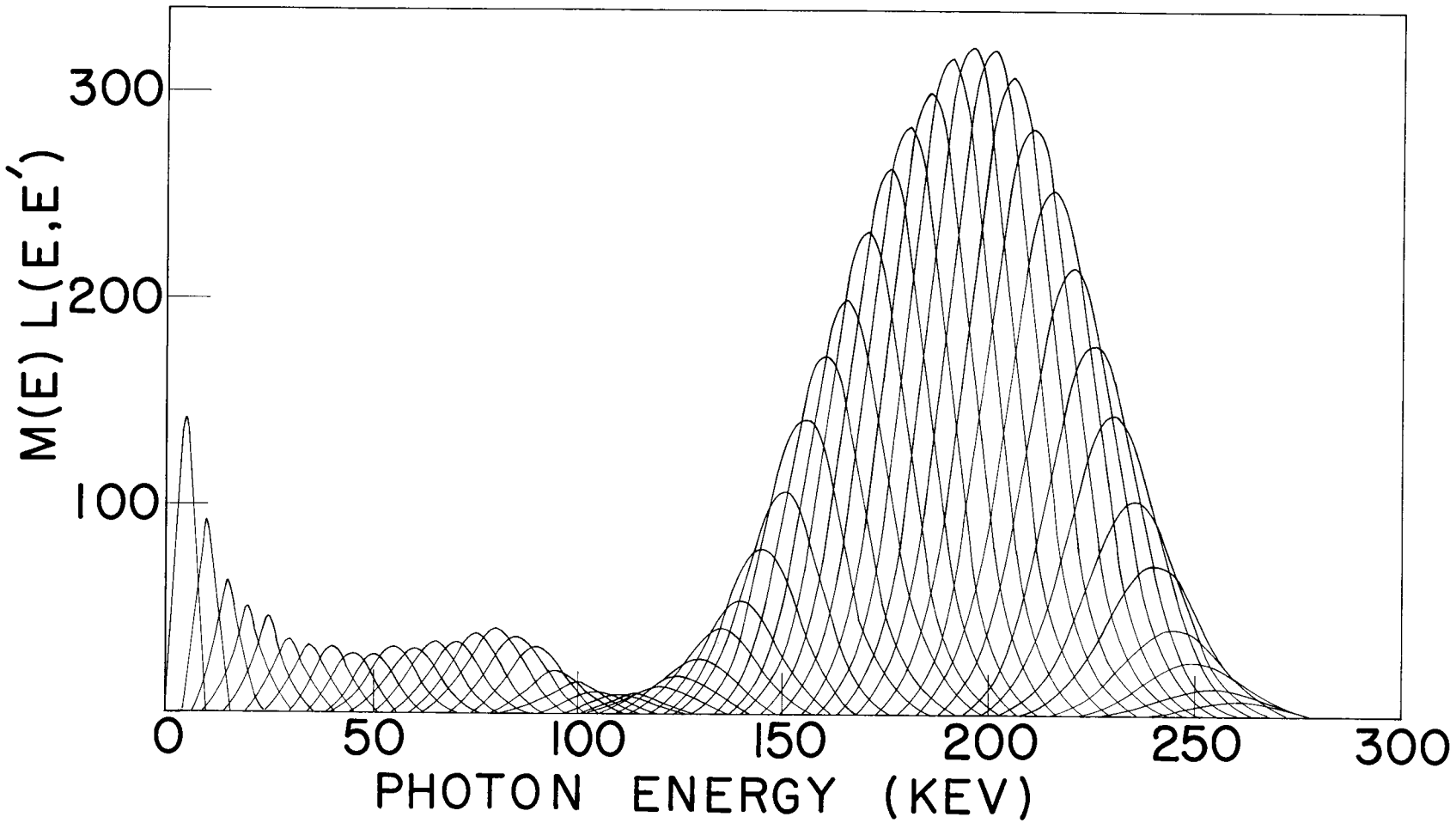

Figure 20. Normalized Gaussians Times the 250 Kev Experimental Spectrum.

$M_1(E) > M(E)$, then $N_1(E) < M(E)$. Thus

$$N_1(E) = M(E) - \left(M_1(E) - M(E) \right)$$
$$= 2\,M(E) - M_1(E) \tag{10}$$

The distribution $M(E)$, $M_i(E)$ and $N_i(E)$ can be seen in Figure 21 for the 250 Kev X-ray spectrum. It will be noted that after the experimental spectrum is multiplied by the Gaussian distribution, the generated curve had a poorer resolution; that is, the peak value is less and the base wider than the experimental spectrum.

The approximate spectrum $N_1(E)$ is then substituted into Equation (8) and a new smeared spectrum $M_2(E)$ is generated. This new spectrum is used as above to produce a second approximation to the true spectrum. In general,

$$N_j = N_{j-1} - (M_j - M) \tag{11}$$

In the problems considered by Freedman, et. al., and in those considered here, the convergence was rapid with only a few iterations being required to determine a spectrum $N(E)$ which when substituted into Equation (8) yielded a spectrum differing from the measured at all energies by 5 per cent or less.

After the corrections for the Gaussian distribution have been removed by the iteration method, the spectrum is still distorted by: 1) the iodine escape peak which is prominent at low energies and

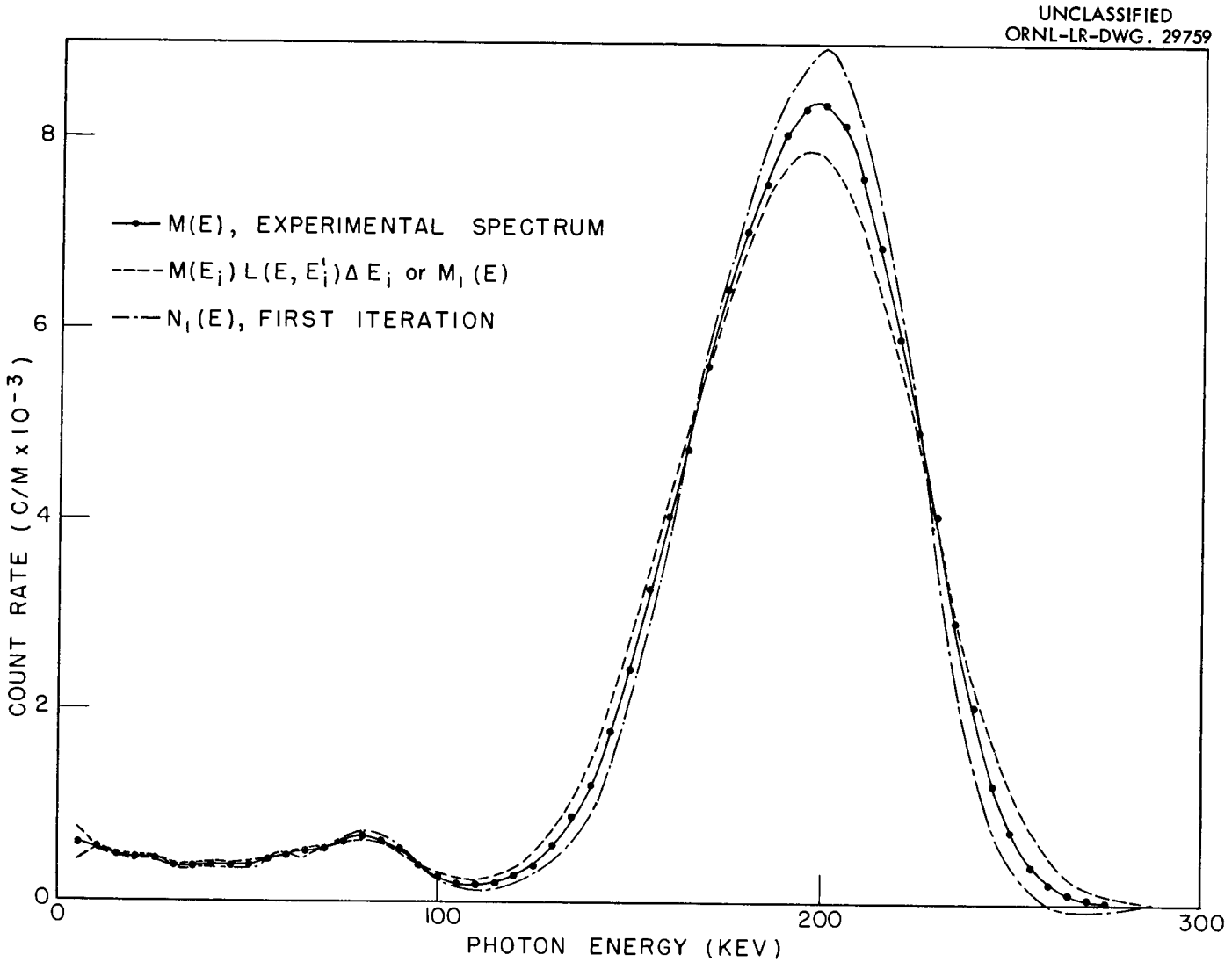

Figure 21. The Effect of the First Iteration on the 250 Kev Experimental Spectrum.

2) the finite probability that an X-ray may pass through the crystal without interacting, which is important at the high energies. The distortion by the iodine escape peak was removed from the iterated experimental spectrum by subtracting the product of the experimental count rate and the "escape ratio" at energy E, from the experimental count rate at energy E — 28.4 Kev. The 28.4 Kev is the energy of the iodine K X-ray which escapes the scintillation crystal. The "escape ratio" is found in the literature and the values used here are from the work by Axel[49] for a system with very good geometry. It will be noted that there is no iodine escape peak for the 30 Kev spectrum because the effective energy of this spectrum is less than the excitation potential needed to produce iodine K X-rays.

To correct for the non-interaction of some of the photons with the crystal, the data available in Figure 1 are used. The fraction of the number of photons that are absorbed at any energy can be calculated from the total absorption cross-section and the thickness of the crystal. This fraction is divided into the iterated experimental count rate at the desired energy to obtain the actual number of photons of a particular energy incident on the crystal. The Compton continuum has been neglected since it is only prominent at energies greater than were used in this experiment. In the experimental 250 Kev spectrum, it was only two per cent of the primary photoelectric peak.

---

[49] Axel, P., op. cit. (footnote 27).

VI. KRAMERS' THEORY

In order to provide a reference for the fully-corrected experimental X-ray spectra, it was decided to compare the distribution to that obtained by Kramers' theory.[50] This theory was proposed in 1923 when Kramers showed on the basis of semi-classical assumptions that the continuous bremsstrahlung spectrum from a thick target could be expressed in a form that may be written as

$$\begin{aligned} I(E)\,dE &= -C(E-Eo)dE, \quad E < Eo \\ &= 0 \qquad\qquad\quad , \quad E > Eo \end{aligned} \tag{12}$$

where $I(E)dE$ is the intensity of the X-rays per unit energy interval E, Eo is the applied voltage, and C is a constant. Combining this result with the usual exponential absorption law and the mass absorption coefficient, the shape of the spectrum can be calculated after transmission through the inherent filtration of the X-ray tube and any added filters:

$$N(E)dE = -C(E-Eo)\prod_i \exp\left\{-\left[\frac{\mu}{\rho}(E)\right]_i \rho_i X_i\right\} \tag{13}$$

In this expression $\frac{\mu}{\rho}(E)_i$ is the mass absorption coefficient of the ith filter of density ρ_i and thickness X_i for incident energy E. The result is a theoretical X-ray distribution which can be compared in

[50] Kramers, H. A., Phil. Mag., 46, 836 (1923).

shape to the corrected experimental spectrum as obtained from the scintillation spectrometer. The results of these comparisons are shown in Figures 22, 23, 24, 25, 26 and 27. The most probable energy -- corresponding to the peak energy -- and the average energy were obtained for each of the theoretical and experimental curves. These energies are given for comparison in Table IV.

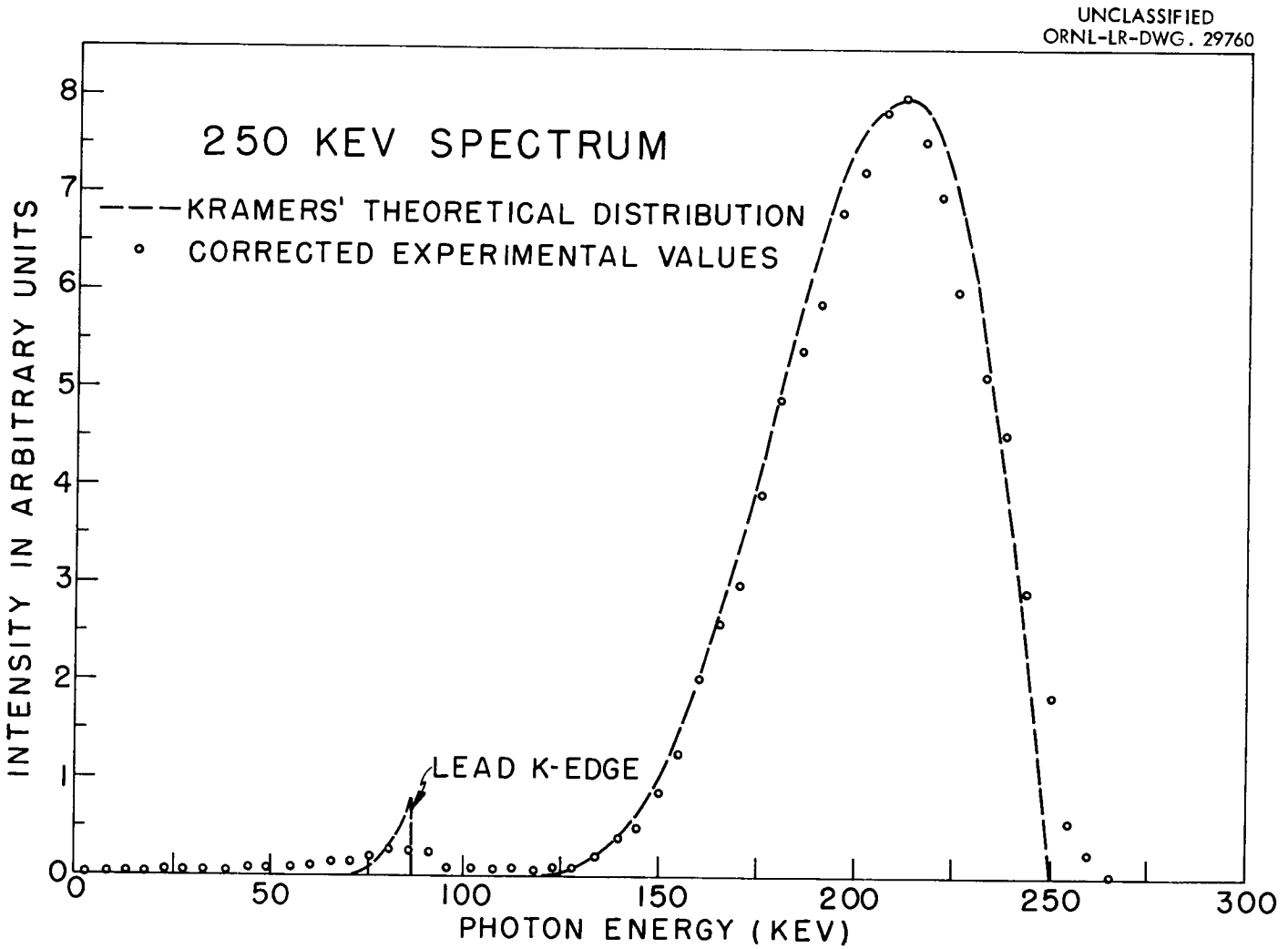

Figure 22. Comparison of Corrected Experimental Values with the Theoretical Kramers' Distribution, 250 Kev Spectrum.

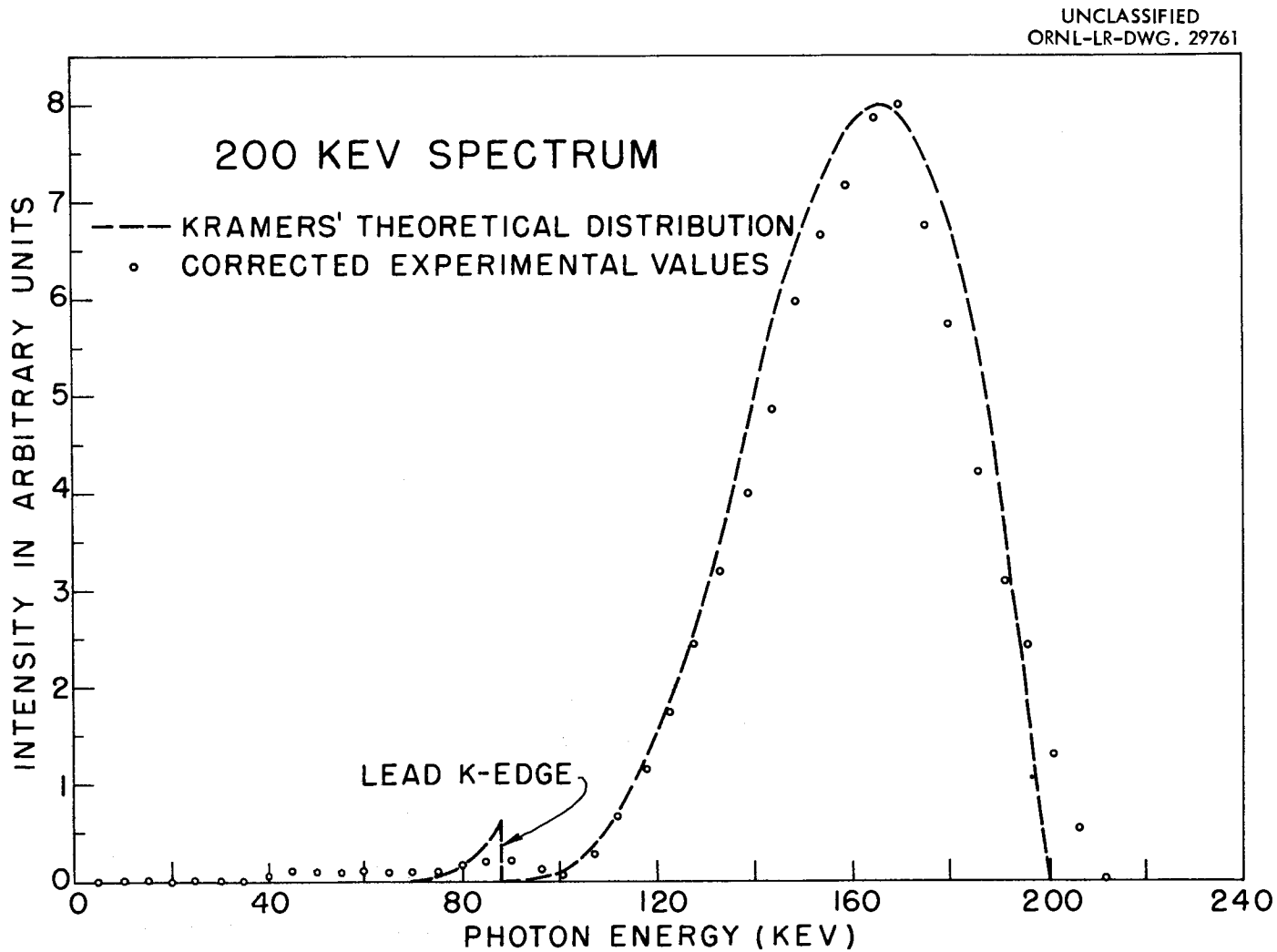

Figure 23. Comparison of Corrected Experimental Values with the Theoretical Kramers' Distribution, 200 Kev Spectrum.

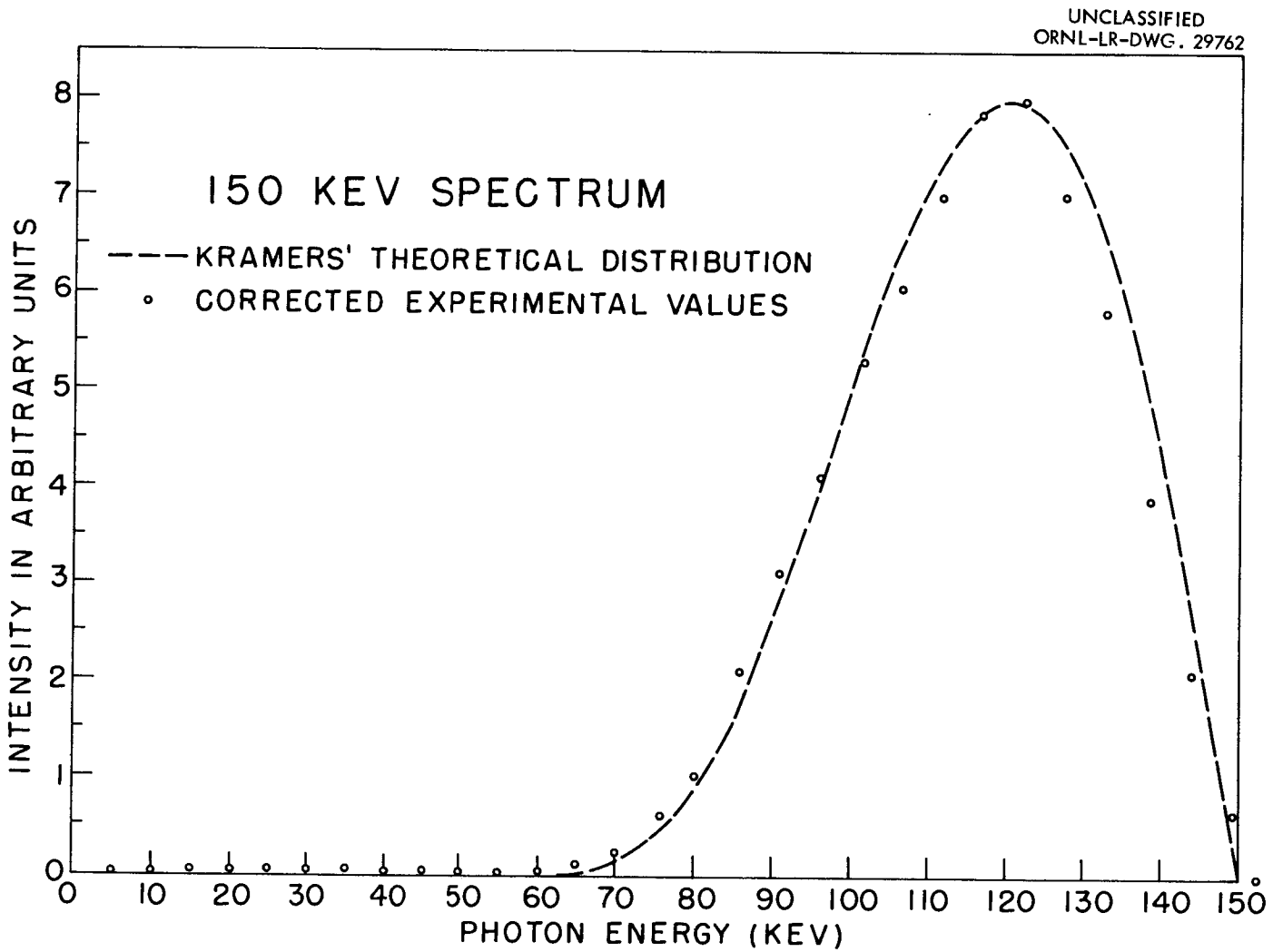

Figure 24. Comparison of Corrected Experimental Values with the Theoretical Kramers' Distribution, 150 Kev Spectrum.

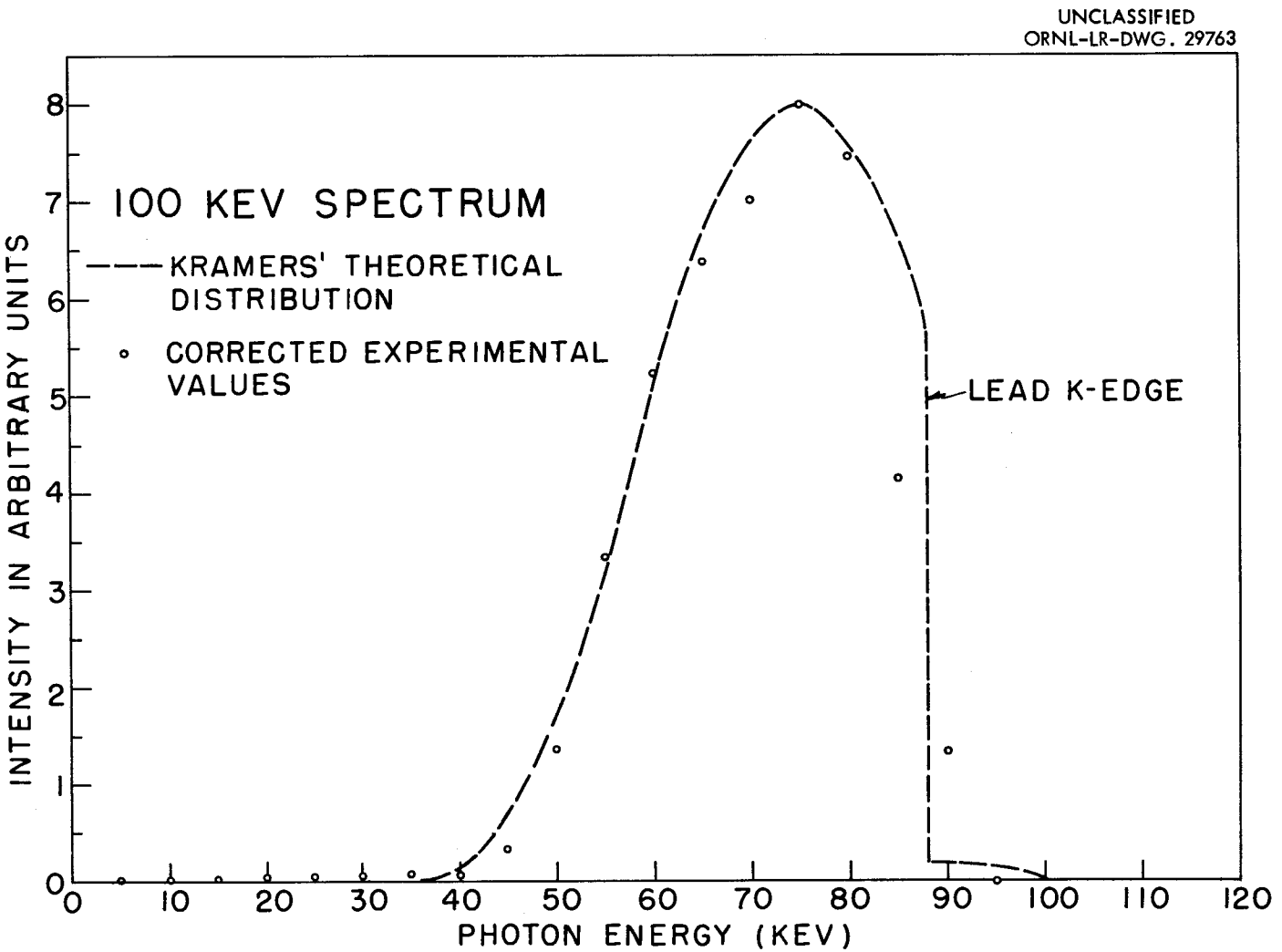

Figure 25. Comparison of Corrected Experimental Values with the Theoretical Kramers' Distribution, 100 Kev Spectrum.

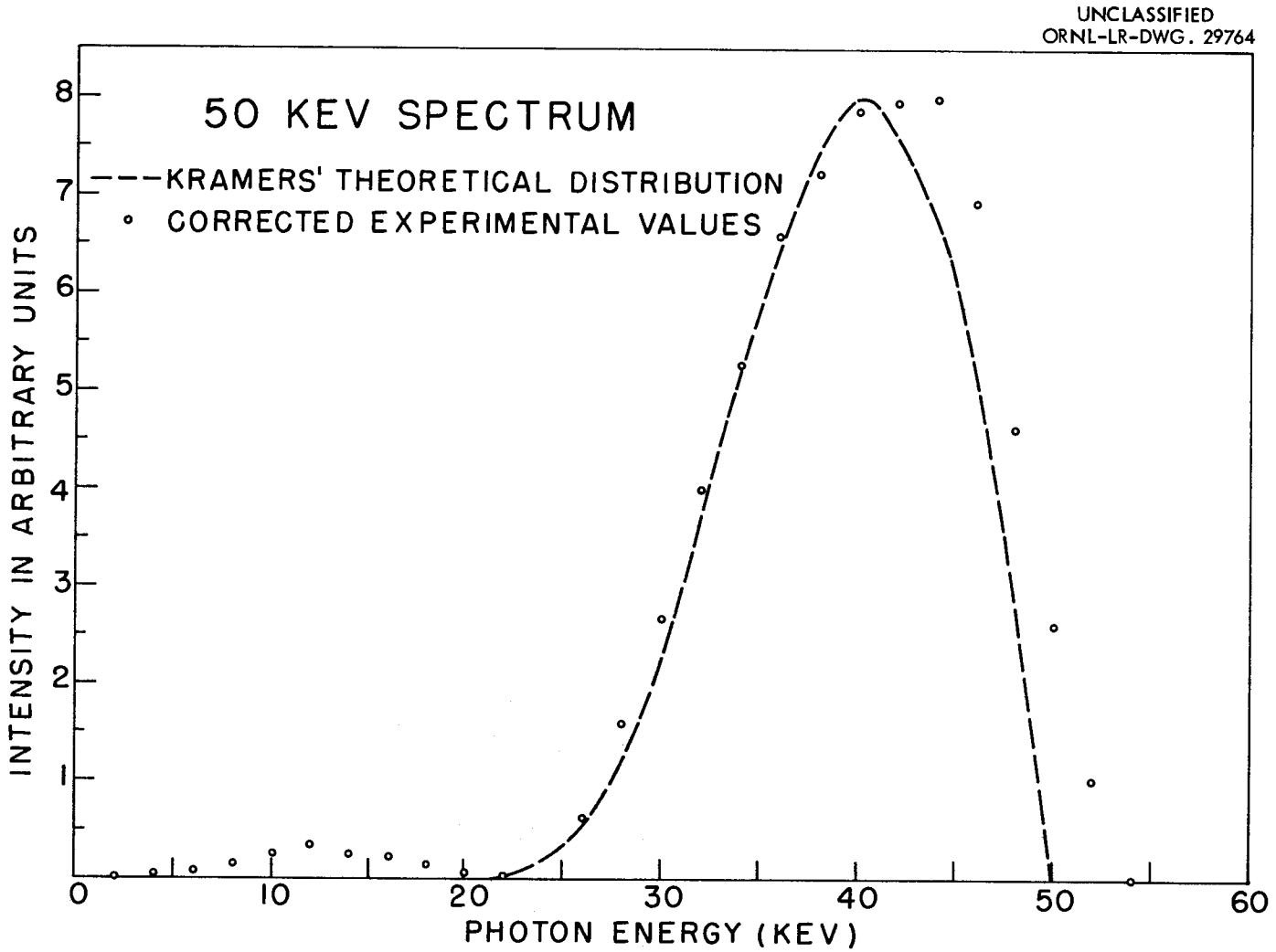

Figure 26. Comparison of Corrected Experimental Values with the Theoretical Kramers' Distribution, 50 Kev Spectrum.

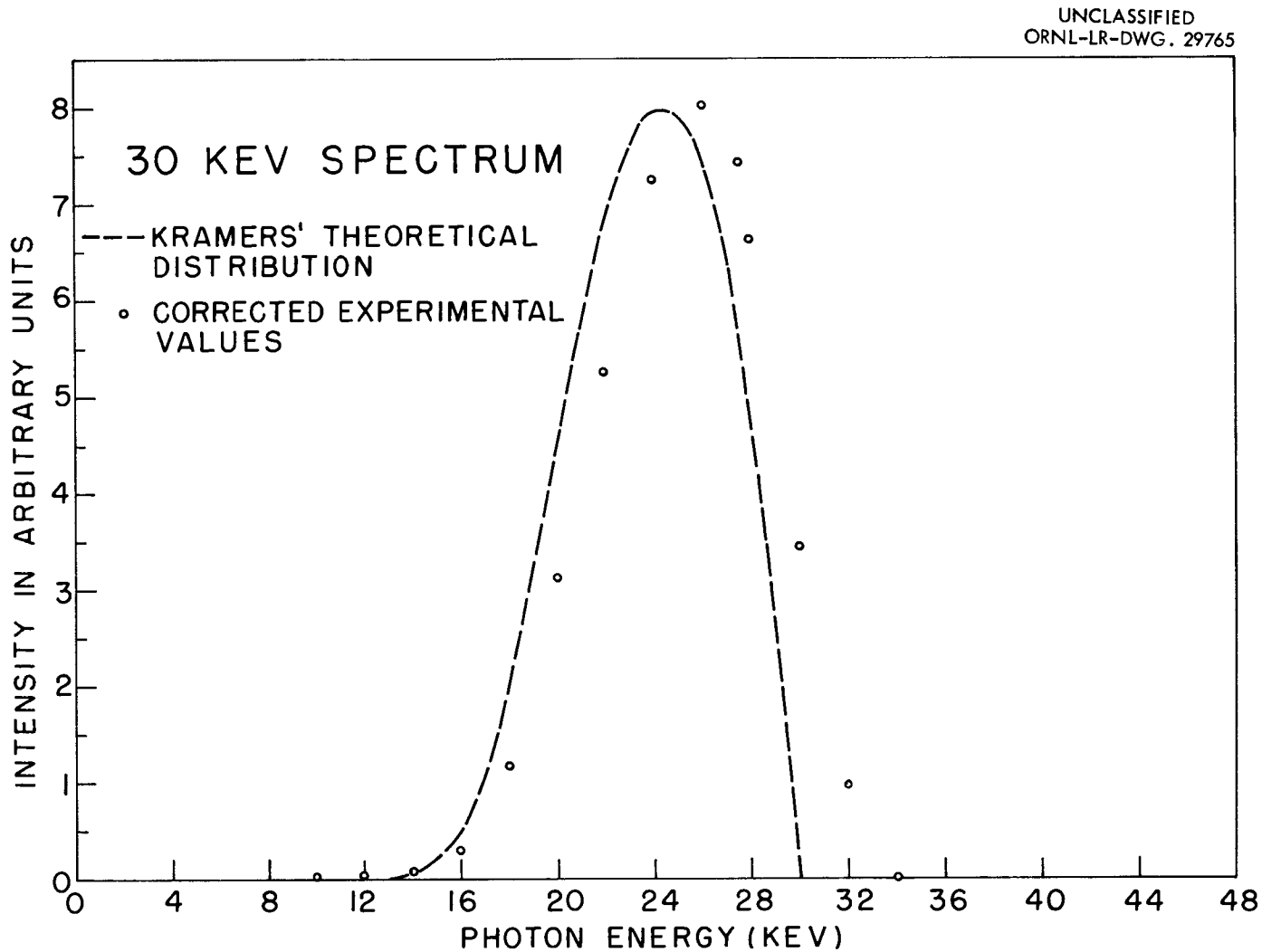

Figure 27. Comparison of Corrected Experimental Values with the Theoretical Kramers' Distribution, 30 Kev Spectrum.

VII. ABSORPTION METHOD

For each spectrum the most probable energy and the average energy may be compared also with the effective energy as obtained by the absorption method. The effective energy is defined as the energy of a monochromatic X-ray beam which would have the same absorption coefficient as the given spectrum in an incremental thickness of standard absorber. To obtain the apparent absorption coefficient the logarithm of the ionization produced by the X-rays in a standard air chamber was plotted as a function of the thickness of a standard filter material. The slope of the tangent to the curve was taken at the thickness corresponding to the regular filter thickness used at that energy. From the slope the absorption coefficient was calculated and the corresponding effective energy obtained from the tables of Grodstein.[51] Absorption runs were made with filters of various thicknesses and atomic numbers, as listed in Table III, and a typical result is shown in Figure 28. The elements chosen as filters were based on the recommendations of the NBS Handbook 62.[52] These filters were analyzed chemically for the presence of extraneous elements with a high atomic number. No significant quantity was found. The results of the effective energies

---

[51] Grodstein, op. cit. (footnote 44).

[52] National Bureau of Standards Handbook 62, Washington D. C., (1956), p. 7.

ORNL-LR-Dwg. 25161
UNCLASSIFIED

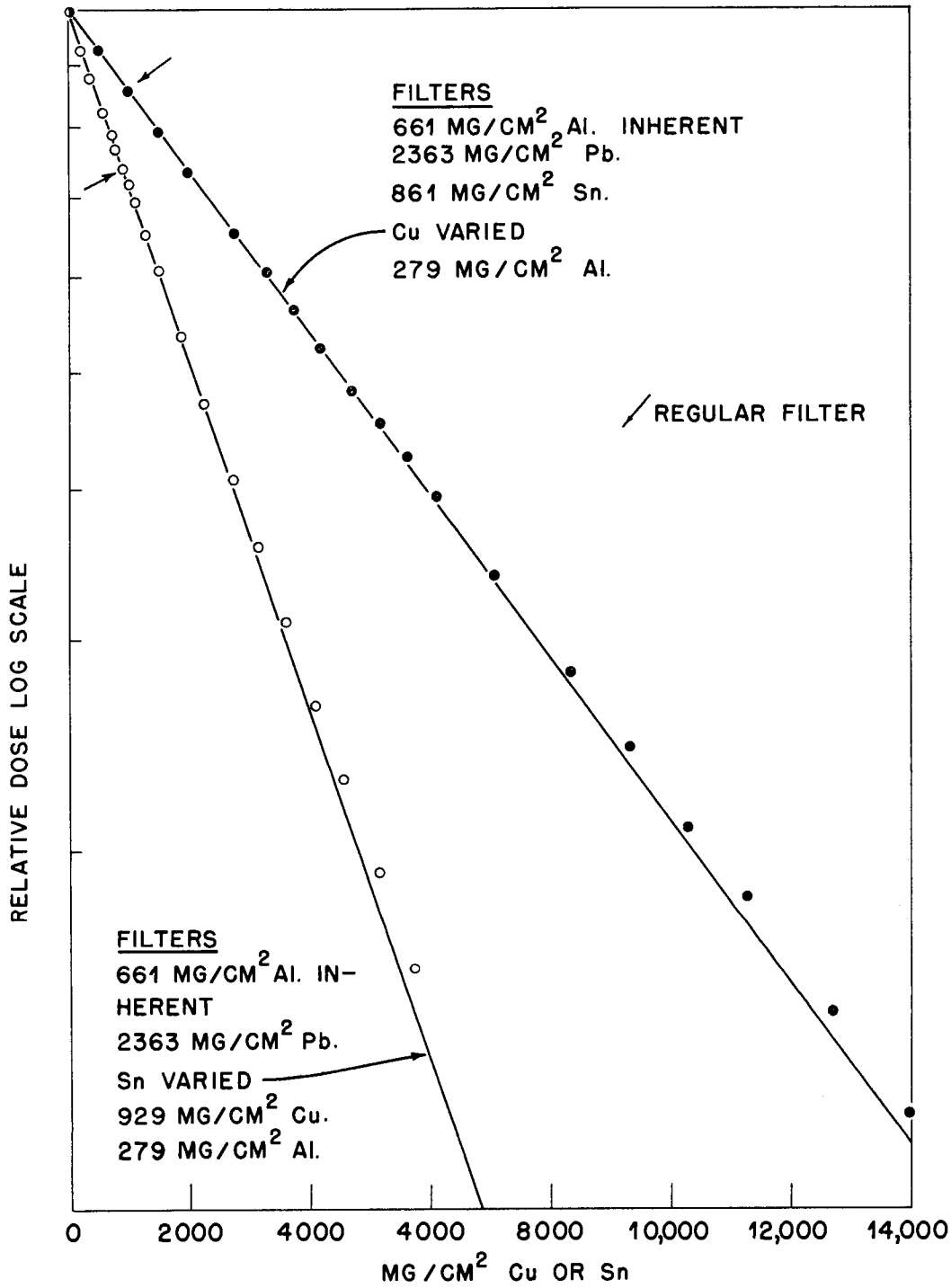

Figure 28. Absorption Curves for the 250 Kev Spectrum.

obtained by the absorption method are shown in Table IV for comparison with the average and most probable energies as determined from the corrected experimental spectra and the Kramers' distribution.

Table IV. Comparison of the Average Energy, Most Probable Energy and the Effective Energy

Approximate X-ray Tube Voltage (Kv)	Average Energy (Kev)		Most Probable Energy (Kev)		Effective Energy (Kev)				Profile Width* (Kev)	
	Corrected Experimental Spectrum	Kramers' Theoretical Distribution	Corrected Experimental Spectrum	Kramers' Theoretical Distribution	Lead Absorbers	Tin Absorbers	Copper Absorbers	Aluminum Absorbers	Corrected Experimental Spectrum	Kramers' Theoretical Distribution
30	25.0	23.6	26	24				22.4	4.4	4.5
50	39.4	39.0	42	40				35.7	8.3	7.4
100	70.5	72.3	75	75			69.0	68.0	14.2	15.3
150	115.2	116.4	123	120			115.5		21.4	22.5
200	159.7	159.5	170	165			158.7		24.7	27.4
250	201.5	201.6	212	215	194.8	196.5	200.9		30.3	32

* Expressed as half width at half-maximum intensity.

VIII. SUMMARY AND DISCUSSION

The energy calibration of the scintillation spectrometer was made by the use of the K X-rays from isotopic decay and fluorescent radiators as well as from gamma energies. However, the preliminary least square curve calibrated from the three gamma ray energies, was used for the 150 Kev, 200 Kev and 250 Kev spectra. It was believed that since the energy of the gamma rays more nearly corresponds to the three high energy X-ray spectra, it was more nearly correct to use the calibration obtained from just the gamma energies than the final calibration curve which includes the low energy fluorescent and isotopic K X-rays.

The resolution calibration of the scintillation spectrometer was also improved by the additional data obtained from the K X-rays. The corrections for the increase in width of the Gaussian distributions due to the superposition of the four lines in the K series cannot be neglected. In the most extreme case (uranium) these K lines could result in an increase in width of 1.53 times the width of a Gaussian from a monoenergetic line at that energy. The selection of filters of appropriate atomic number to reduce the intensity of the K_β lines reduced the line profile width for the fluorescent X-rays. The filter materials that were available only in powder form were mixed with a self-hardening liquid plastic. This procedure facilitated easy handling of the filters and provided a simple method for making the filters in any desired thickness.

Six filtered X-ray energy distributions were chosen for the comparison of the experimental spectra with the theoretical spectra. The voltages applied to the X-ray tube were 30, 50, 100, 150, 200 and 250 Kv. Table III lists the desired X-ray energies, the voltage dial settings and the observed voltages.

The data available from the resolution calibration were used in correcting the experimental spectra by an iterative method. Thus, the distortions which resulted from the Gaussian line profile were largely removed from the spectra. After application of this correction, the peak count rate was increased and the width of the curve decreased, as would be expected. After the first iteration, the difference between $\left[M_1(E) - M(E) \right]$ and the experimental values M(E) as shown in Equation 10 was a maximum of 9% of the experimental spectrum. This difference decreased to a maximum of 4% after the second iteration, indicating that distortion was much reduced.

Experimentally determined points which were subject to statistical fluctuations were used as input data in the iteration instead of values taken from a smooth curve drawn through the experimental distribution. Since the iteration tends to accentuate slight fluctuations such as arise statistically, the final iteration (usually the second one except for the 250 Kev spectrum where three iterations were used) magnifies the errors of the "bad" points. Another peculiarity of the iteration process is the negative values that arise, particularly at the high energy end of the spectrum as a result of the over-correction of the count rate. This effect can be seen in Figure 21.

In the successive iterations the negative values tend to converge toward zero count rate. They were carried throughout the iterations because their removal would have introduced errors in adjacent positive points. These values were assumed to be zero when the corrected experimental spectra were compared to the theoretical X-ray distributions since they amounted only to approximately 2.5% of the peak count rate.

Corrections for efficiency of the crystal and for iodine escape were small and amounted to a few percent of the count rate, except in the 50 Kev spectrum where the iodine escape peak corresponded to a maximum of about 24% of the count rate. This occurs just above the 33 Kev K-absorption edge of iodine. No corrections other than the iteration were needed for the 30 Kev spectra because the energy was not high enough to produce iodine escape and was low enough to permit 100% absorption in the crystal. The escape of Compton scattered radiation is negligible in this work.

The corrected experimental intensity spectra agree with the Kramers theoretical distribution, except in the 30 Kev spectrum where the experimental distribution appears displaced. This is probably the result of variations in the calibration of the scintillation spectrometer which becomes more critical at low energies. The lead K-edge peaks in the 250 Kev and 200 Kev spectra are the result of the "transparency" of the lead in the X-ray filters to energies just below the 88 Kev lead K-absorption edge.

The average energies, most probable energies and effective energies as shown in Table IV give surprisingly close agreement, except for the 30 Kev and 50 Kev data. The agreement of the remaining four spectra is within 3.5% which is unusual, considering there is an approximate 2% fluctuation in the incident X-ray beam during the collecting time for the data for one distribution.

APPENDIX I

Sample of Least Squares Calculation

Least squares fits were made to the data plotted in Figures 8, 10, 17, 18 and 28 as well as to the data obtained by the absorption method listed in Table IV. A typical example is included here of the data plotted in Figure 18 obtained on Gain 2. Let the equation of line be $y = c + dx$, where y is a^2, and x is the corresponding photon energy, and c and d are constants given by

$$c = \frac{\Sigma x_n^2 \; \Sigma y_n - \Sigma x_n \; \Sigma (x_n y_n)}{K \Sigma x_n^2 - (\Sigma x_n)^2},$$

and

$$d = \frac{K \Sigma (x_n y_n) - \Sigma x_n \Sigma y_n}{K \Sigma x_n^2 - (\Sigma x_n)^2}$$

Omitting the details,

$$K = 12$$

$$\Sigma x_n = 1.0959 \times 10^3$$

$$\Sigma y_n = 1.2097 \times 10^3$$

$$\Sigma x_n^2 = 1.53056 \times 10^5$$

$$(\Sigma x_n)^2 = 1.20099 \times 10^6$$

$$\Sigma (x_n y_n) = 1.65946 \times 10^5$$

Using these values to calculate c and d, the equation of the line is

$$y = 5.17 + 1.0471\ x$$

Since the resolution at zero energy should be zero, the least square fit would be more accurately represented by the equation y = dx where the constant d is given by

$$d = \frac{\Sigma\ (x_n y_n)}{\Sigma\ x_n^{\ 2}}$$

and the constant c = 0. This particular fit was only made for the data in Figure 18. Omitting the details, the equation of the line is

$$y = 1.0842\ x$$

In order to confirm the fact that the line should go through the origin, a statistical analysis was applied to determine if there was any significance in the difference between the observed intercept of 5.17 and the origin. The "t" test was used to determine this significance and involves the "t" value obtained from the ratio of the difference between intercepts (5.17 - 0) and the residual variance of the intercept. If the "t" value indicates there is no significance in the difference between

intercepts, it may be concluded that the equation of the line may be represented by

$$y = 1.0842\ x$$

The residual variance S^2 is expressed as

$$S^2 = \frac{\Sigma\ (y_n-\bar{y})^2 - d\ \Sigma\ (x_n-\bar{x})\ (y_n-\bar{y})}{K - 2},$$

and the residual variance of the intercept $S_c^{\ 2}$ as[53]

$$S_c^{\ 2} = \frac{S^2\ \ \Sigma\ x_n^{\ 2}}{K\ \Sigma\ (x_n-\bar{x})^2}$$

where

$$\Sigma\ (x_n-\bar{x})^2 = 5.2972 \times 10^4$$

$$\Sigma\ (y_n-\bar{y})^2 = 5.9010 \times 10^4$$

$$\Sigma\ (x_n-\bar{x})(y_n-\bar{y}) = 5.5470 \times 10^4$$

The residual variance of the intercept (S_c) is 22.316 and therefore the value of "t" is from the equation

$$t = \frac{d-o}{S_c} = \frac{5.17}{4.62} = 1.12$$

---

53 Youden, W. J., STATISTICAL METHODS FOR CHEMISTS, (John Wiley and Sons, New York, 1951) p. 43.

Looking up in the table of t[54] under 10 degrees of freedom (K-2), the probability of a larger value of "t" occurring is found to be 0.29. This means that one would be wrong 29% of the time in saying that the difference between 5.17 and 0 was real. This is too high a percentage to be significant as the usual limit in the "t" test is 5%. Therefore, it can be concluded that the equation $y = 1.0842\ x$ is a legitimate fit to the experimental points.

---

[54] Snedecor, G. W., STATISTICAL METHODS, (The Iowa State College Press, Ames, Iowa, 1946) p. 65.

Bibliography

Axel, P., "Escape Peak Correction to Gamma-Ray Intensity Measurements Made With Sodium Iodide Crystals," BNL-271(T-44), Brookhaven Nat. Lab., Upton, New York (1953). Unpublished.

Beach, L. A., Theus, R. B., and Faust, W. R., NRL Report 4277, (1953) Unpublished.

Bell, G. E., "Spectral Distribution in the Continuous X-ray Spectrum and the Specification of X-ray Quality," Brit. J. Rad. 9, 680, (1936).

Bell, P. R., "The Use of Anthracene as a Scintillation Counter," Phys. Rev. 73, 1405 (1948).

"The Biological Effects of Atomic Radiation," Report of the Committee on Genetic Effects, National Academy of Sciences, National Research Council, Washington (1956) p. 29 of Summary Reports.

Blaw, M., and Dreyfus, B., "The Multiplier Photo-Tube in Radioactive Measurements," Rev. Sci. Instr. 16, 245 (1945).

Breitenberger, E., PROGRESS IN NUCLEAR PHYSICS, (Frisch ed. - Pergammon Press, New York, 1955) Vol. 4, Chapter 2.

Compton, A. H., and Allison, S. K., X-RAYS IN THEORY AND EXPERIMENT, (D. Van Nostrand Co., Inc., New York, 1935).

Cormack, D. V., Till, J. E., Whitmore, G. F., and Johns, H. E., "Measurement of Continuous X-ray Spectra with a Scintillation Spectrometer," Brit. J. Rad., 28, 605 (1955).

Duane, W., "The Character of the General, or Continuous Spectrum Radiation," Proc. Nat. Acad. Sci. U. S., 13, 662 (1927).

Ehrlich, M., "Scintillation Spectrometry of Low-Energy Bremsstrahlung," J. Research Natl. Bur. Standards, 54, No. 2, 107 (1955).

Ehrlich, M., and Fitch, S. H., "Photographic X- and Gamma-Ray Dosimetry," Nucleonics, 9, No. 3, p. 5 (Sept., 1951).

Ehrlich, M., "Narrow Band Spectra of Low-Energy X-Radiation," Radiation Research 3, 223A (1955).

Fine, S., and Hendee, C. F., "X-Ray Critical-Absorption and Emission Energies in Kev," Nucleonics, 13, No. 3, p. 36 (March, 1955).

Freedman, M. S., Novey, T. B., Porter, F. T., and Wagner, F., "Correction for Phosphor Backscattering in Electron Scintillation Spectrometry," Rev. of Sci. Instr., 27, 716 (1956).

Glasser, O., Quimby, E. H., Taylor, L. S., and Weatherwax, J. L., PHYSICAL FOUNDATIONS OF RADIOLOGY, (Paul B. Hoeber, Inc., New York, Second edition, 1952).

Greenfield, M. A., Specht, R. D., Kratz, P. M., and Hand, K., "Spectral Energy Distribution in X-ray Beam as a Function of Wavelength," J. Opt. Soc. Am., 42, 6 (1952).

Greening, J. R., "The Determination of the X-Ray Energy Distributions by the Absorption Method," Brit. J. Rad., 20, 71 (1947).

Grodstein, G. W., "X-Ray Attenuation Coefficients from 10 Kev to 100 Mev," Natl. Bur. Standards Circular 583, (1957), Wash., D. C.

Heitler, W., THE QUANTUM THEORY OF RADIATION, (Oxford University Press, Third edition, 1954).

Hofstadter, R., "Alkali Halide Scintillation Counters," Phys. Rev. 74, 100 (1948).

Hofstadter, R., "The Detection of Gamma-Rays with Thallium-Activated Sodium Iodide Crystals," Phys. Rev. 75, 796 (1949).

Hollander, J. M., Perlman, I., and Seaborg, G. T., "Table of Isotopes," Rev. of Modern Phys., 25, 613 (1953).

Hull, A. W., "The X-Ray Spectrum of Tungsten," Gen. Elec. Rev., 19, 603 (1916).

Johansson, S. A. E., "The Use of Scintillation Counters in the Measurement of the Energy of X-Rays and Low Energy Gamma Rays," Arkiv för Fysik, 3, 533 (1952).

Johnston, L. W., Birkhoff, R. D., Cheka, J. S., Hubbell, H. H. Jr., and Saunders, B. G., "Response of the Anthracene Scintillation Counter to Low-Energy Electrons," ORNL-2298, Oak Ridge, Tenn., (1957); Rev. Sci. Instr. 28, 765 (1957).

Jones, D. E. A., "The Determination from Absorption Data of the Distribution of X-Ray Intensity in the Continuous X-Ray Spectrum," Brit. J. Rad., 13, 95 (1940).

Kramers, H. A., "On the Theory of X-Ray Absorption and of the Continuous X-Ray Spectrum," Phil. Mag., 46, 836 (1923).

Kulenkampff, H., "Uber Das Kontinuierliche Röntgenspektrum," Ann. Physik, 69, 548 (1922).

Kulenkampff, H., "Untersuchungen Der Kontinuierlichen Röntgenstrahlung Dünner Aluminiumfoilen," Ann. Physik, 87, 597 (1928).

Larson, H. V., Myers, I. T., and Roesch, W. C., "A Wide Beam Fluorescent X-Ray Source," HW-31781 (1954) Hanford Atomic Products Operation, Richland, Washington. Unpublished.

Liden, K., and Starfelt, N., "Scintillation Spectrometry of Continuous γ- and X-Ray Spectra Below 1 Mev," Ark. F. Fys., 7, 427 (1954).

Madansky, L., and Rasetti, F., "Continuous Radiation of β Emitters," Phys. Rev., 83, 187 (1951).

McGowan, F. K., "Measure of K-Shell Internal Conversion Coefficients With a Coincidence Scintillation Spectrometer," Phys. Rev., 93, 163 (1954).

National Bureau of Standards Handbook 62, Report of the International Commission on Radiological Units and Measurements (ICRU), Washington, D. C., (1956).

Nicholas, W., "Continuous Spectrum X-Rays from Thin Targets," J. Research Natl. Bur. Standards, 2, 837 (1929).

Ramm, W. J., and Stein, M. N., "Spectral Distribution of Filtered X-Ray Beams," Phys. Rev., 92, 1081A (1953).

Schubert, J., and Lapp, R. E., RADIATION: WHAT IT IS AND HOW IT AFFECTS YOU, (The Viking Press, Inc., New York, 1957).

Seemann, H. E., "Spectral Sensitivity of Two Commercial X-Ray Films Between 0.2 and 2.5 Angstroms," Rev. Sci. Instr. 21, 314 (1950).

Sharpe, J., NUCLEAR RADIATION DETECTORS, (John Wiley and Sons, Inc., New York, 1955), pp. 101-107.

Silberstein, L., "Determination of the Spectral Composition of X-Ray Radiation from Filtration Data," J. Opt. Soc. Am., 22, 265 (1932).

Snedecor, G. W., STATISTICAL METHODS, (Iowa State College Press, Ames, Iowa, 1946).

Taylor, S., "The Determination of the X-Ray Quality by Filter Methods," Radiology, 29, 22 (1937).

Ulrey, C. T., "An Experimental Investigation of the Energy in the Continuous X-Ray Spectra of Certain Elements," Phys. Rev., 11, 401 (1918).

Victoreen, J. A., "The Calculation of X-Ray Mass Absorption Coefficients," J. Appl. Phys., 20, 1141 (1949).

Wang, P. K. S., Raridon, R. J., and Crawford, R. C., "X-Ray Spectrum from a Beryllium Window Tube," Brit. J. Rad., 30, 153 (1957).

Webster, D. L., "X-Ray Emissivity as a Function of Cathode Potential," Phys. Rev. 9, 220 (1917).

Youden, W. J., STATISTICAL METHODS FOR CHEMISTS, (John Wiley and Sons, Inc., New York, 1951).

ORNL-2529
Physics and Mathematics
TID-4500 (13th ed., Rev.)
February 15, 1958

INTERNAL DISTRIBUTION

1. C. E. Center
2. Biology Library
3. Health Physics Library
4-5. Central Research Library
6. Reactor Experimental Engineering Library
7-26. Laboratory Records Department
27. Laboratory Records, ORNL R.C.
28. L. B. Emlet (K-25)
29. J. P. Murray (Y-12)
30. A. M. Weinberg
31. J. A. Swartout
32. E. D. Shipley
33. M. L. Nelson
34. K. Z. Morgan
35. S. C. Lind
36. A. S. Householder
37. C. S. Harrill
38. C. E. Winters
39. A. H. Snell
40. E. H. Taylor
41. W. H. Jordan
42. T. A. Lincoln
43. A. Hollaender
44. F. L. Culler
45. H. E. Seagren
46. D. Phillips
47. M. T. Kelley
48. E. E. Anderson
49. R. S. Livingston
50. C. P. Keim
51. K. E. Cowser
52. C. D. Susano
53. L. B. Farabee
54. F. J. Davis
55. R. J. Morton
56. C. E. Haynes
57. E. G. Struxness
58. W. E. Cohn
59-109. H. H. Hubbell, Jr.
110. D. E. Arthur
111. J. Neufeld
112. M. J. Skinner
113. J. C. Hart
114. T. H. J. Burnett
115. W. J. Lacy
116. G. S. Hurst
117. T. E. Bortner
118. J. A. Lane
119. H. P. Yockey
120. C. E. Clifford
121. J. L. Gabbard
122. R. A. Charpie
123. G. E. Boyd
124. D. M. Davis
125. P. E. Brown
126. E. D. Gupton
127. J. C. Ledbetter
128. R. L. Clark
129. C. C. Cain
130. L. C. Johnson
131. W. W. Ogg
132. O. D. Teague
133. E. L. Sharp
134. E. J. Kuna
135. H. H. Abee
136. C. R. Guinn
137. A. D. Warden
138. C. C. Sartain
139. J. R. Muir
140. J. A. Auxier
141. M. F. Fair
142. S. I. Auerbach
143. G. W. Royster, Jr.
144. R. R. Dickison
145. F. W. Sanders
146. F. C. Maienschein
147. W. J. Boegly, Jr.
148. F. L. Parker
149. W. E. Lotz
150. B. Fish
151. M. B. Edwards
152. F. M. Empson
153. G. G. Robeck
154-204. R. D. Birkhoff
205. R. H. Ritchie
206. J. A. Harter
207. W. G. Stone
208. J. S. Cheka
209. P. N. Hensley
210. R. W. Peelle
211-261. J. C. Villforth
262. E. B. Wagner
263. C. A. Preskitt

264. ORNL - Y-12 Technical Library, Document Reference Section
265. S. K. Allison (consultant)
266. W. H. Langham (consultant)
267. A. Wolman (consultant)
268. R. Zirkle (consultant)
269. L. S. Taylor (consultant)
270. F. H. W. Noll (consultant)

EXTERNAL DISTRIBUTION

271. S. C. Sigoloff, USAF, The Radiobiological Laboratory, University of Texas, Austin, Texas
272-275. Commandant, US Air Force Institution of Technology, Wright-Patterson Air Force Base, Ohio
276-278. J. F. Pierce, Preventive Medicine Division, Office of the Surgeon General, Dept. of the Air Force, Hdqts., USAF, Washington 25, D. C.
279-281. J. C. Carmichael, Office of the Surgeon, Hdqts., Air Material Command, Wright-Patterson Air Force Base, Ohio
282. J. I. Hopkins, Physics Department, Vanderbilt University, Nashville, Tenn.
283. D. G. Yerg, Physics Department, Michigan School of Mines, Houghton, Mich.
284. M. Ehrlich, National Bureau of Standards, Washington 25, D. C.
285. W. J. Ramm, Chief, Nucleonics Section, Physics Research Branch, Hdqts., Signal Corps Eng. Laboratory, Fort Monmouth, N. J.
286. D. V. Cormack, Physics Department, University of Saskatchewan, Saskatton, Saskatchewan, Canada
287. R. Rohrer, Emory Univesity, Department of Physics, Atlanta, Ga.
288. Division of Research and Development, AEC, ORO
289-892. Given distribution as shown in TID-4500 (13th ed., Rev., Feb. 15, 1958) under Physics and Mathematics category (75 copies - OTS)